Limited release of previously-frozen C and increased new peat formation after thaw in permafrost peatlands

Cristian Estop-Aragonés[a,*], Mark D.A. Cooper[a], James P. Fisher[b], Aaron Thierry[c],
Mark H. Garnett[d], Dan J. Charman[a], Julian B. Murton[e], Gareth K. Phoenix[b], Rachael Treharne[b],
Nicole K. Sanderson[a], Christopher R. Burn[f], Steve V. Kokelj[g], Stephen A. Wolfe[f,h],
Antoni G. Lewkowicz[i], Mathew Williams[c], Iain P. Hartley[a]

[a] Geography, College of Life and Environmental Sciences, University of Exeter, Rennes Drive, Exeter, EX4 4RJ, UK
[b] Department of Animal & Plant Sciences, University of Sheffield, Western Bank, Sheffield, S10 2TN, UK
[c] School of GeoSciences, University of Edinburgh, Edinburgh, EH9 3FF, UK
[d] NERC Radiocarbon Facility, Scottish Enterprise Technology Park, Rankine Avenue, East Kilbride, G75 OQF, UK
[e] Department of Geography, University of Sussex, Brighton, BN1 9QJ, UK
[f] Department of Geography and Environmental Studies, Carleton University, Ottawa, Ontario, K1S 5B6, Canada
[g] Northwest Territories Geological Survey, Government of the Northwest Territories, Yellowknife, NWT, Canada
[h] Geological Survey of Canada, Natural Resources Canada, Ottawa, Ontario, K1A 0E8, Canada
[i] Department of Geography, Environment and Geomatics, University of Ottawa, Ottawa, Ontario, K1N 6N5, Canada

ARTICLE INFO

ABSTRACT

Permafrost stores globally significant amounts of carbon (C) which may start to decompose and be released to the atmosphere in form of carbon dioxide (CO_2) and methane (CH_4) as global warming promotes extensive thaw. This permafrost carbon feedback to climate is currently considered to be the most important carbon-cycle feedback missing from climate models. Predicting the magnitude of the feedback requires a better understanding of how differences in environmental conditions post-thaw, particularly hydrological conditions, control the rate at which C is released to the atmosphere. In the sporadic and discontinuous permafrost regions of north-west Canada, we measured the rates and sources of C released from relatively undisturbed ecosystems, and compared these with forests experiencing thaw following wildfire (well-drained, oxic conditions) and collapsing peat plateau sites (water-logged, anoxic conditions). Using radiocarbon analyses, we detected substantial contributions of deep soil layers and/or previously-frozen sources in our well-drained sites. In contrast, no loss of previously-frozen C as CO_2 was detected on average from collapsed peat plateaus regardless of time since thaw and despite the much larger stores of available C that were exposed. Furthermore, greater rates of new peat formation resulted in these soils becoming stronger C sinks and this greater rate of uptake appeared to compensate for a large proportion of the increase in CH_4 emissions from the collapse wetlands. We conclude that in the ecosystems we studied, changes in soil moisture and oxygen availability may be even more important than previously predicted in determining the effect of permafrost thaw on ecosystem C balance and, thus, it is essential to monitor, and simulate accurately, regional changes in surface wetness.

1. Introduction

Soils in the northern circumpolar permafrost region (17.8×10^6 km^2, 0–3 m depth) represent the largest terrestrial carbon store, containing > 1000 Pg C (Hugelius et al., 2014; Tarnocai et al., 2009), which has accumulated over thousands of years (Gorham et al., 2007; Harden et al., 1992; Mackay, 1958; Zoltai, 1995). Permafrost peatlands (histels) occupy more than 1 million km^2 in lowlands of the

Arctic and Subarctic and, with thick organic soil horizons, contain disproportionally high amounts of soil carbon per unit area (Hugelius et al., 2014). In uplands and well-drained landscapes, gelisols have thinner organic soil horizons (orthels and turbels) but constitute an even larger stock globally due to their ∼7 times greater spatial extent (Hugelius et al., 2014). Although more than half of this C stock is perennially frozen (Hugelius et al., 2014; Tarnocai et al., 2009), a substantial fraction may thaw this century (Brown and Romanovsky,

2008; Camill, 2005; Harden et al., 2012), decompose and enter the atmosphere as CO_2 or CH_4, potentially exacerbating climate change (Schuur et al., 2015). This permafrost carbon feedback is missing in Earth system models (Ciais et al., 2013) and its inclusion may result in high-latitude ecosystems being predicted to become sources rather than sinks of C during the 21st century (Koven et al., 2011). However, the magnitudes and timings of soil organic carbon (SOC) loss from permafrost are highly uncertain, with estimates of 37–347 Pg C by 2100 (Schaefer et al., 2014). Changes in vegetation and soil C storage are also predicted to have increased in the last decades in the permafrost region and need to be considered along with the loss of permafrost SOC (McGuire et al., 2016). Thus, accurately projecting future rates of CO_2 release from permafrost is essential for predicting the magnitude of this feedback.

The impacts of permafrost thaw at the landscape level strongly depend on the terrain topography and ground-ice characteristics, which influence drainage and moisture conditions in the newly-thawed soils (Jorgenson and Osterkamp, 2005; Osterkamp et al., 2000). In upland and well-drained areas, thaw typically results in deepening of the active layer and as water drains from the system, oxic conditions tend to predominate throughout the soil profile. In contrast, thaw in peatlands that have developed in lowlands with ice-rich permafrost often results in thermokarst landforms characterized by surface subsidence, water-logging, vegetation change and fast peat accumulation following thaw (Beilman, 2001; Camill, 1999; Turetsky et al., 2007, 2000; Zoltai, 1993). Soil moisture strongly controls the type of decomposition (aerobic vs anaerobic) through the oxygen content in the soil and thus the amount and form (CO_2 and CH_4) of C released (Elberling et al., 2011; Estop-Aragonés et al., 2012; Schädel et al., 2016). A recent analysis of laboratory incubation data suggested that the rates of C release will be greater, and have more effect on the climate, if thaw results in oxic (release as CO_2) rather than anoxic conditions, even after accounting for the potential release of the more powerful greenhouse gas CH_4 under anoxic conditions (Schädel et al., 2016). However, in situ observations of changes in ecosystem C storage in Alaska suggest that under anoxic conditions the potential still exists for rapid (within decades) C losses equating to 30–50% of peat plateau C stocks following thaw (Jones et al., 2016; O'Donnell et al., 2012). Given this uncertainty, there is an urgent requirement for in situ quantification of rates of previously-frozen C release following thaw in contrasting ecosystems.

Critically, there are no reported measurements of rates of CO_2 release from previously-frozen C following either fire-induced thaw in well-drained forests or thermokarst in peatland plateaus, despite the large spatial extent of these disturbances in the Boreal (Grosse et al., 2011). While permafrost thaw in peatlands can result in clear changes within the ecosystem, thaw in well-drained sites without ice-rich permafrost can be much harder to detect in the landscape. Forest fires, whose frequency and severity have increased during recent decades (Gillett et al., 2004; Kasischke et al., 2010), remove vegetation and surface organic matter, which are important controls on the ground surface energy balance. This can result in rapid warming and substantial deepening of the active layer in uplands and well-drained areas (Burn, 1998; Fisher et al., 2016; Yoshikawa et al., 2002). Thus, paired burnt and unburnt sites offer an opportunity to quantify potential rates of release of previously-frozen C under oxic conditions. Furthermore, as permafrost C is typically thousands of years old (Gorham et al., 2007; Harden et al., 1992; Mackay, 1981; Zoltai, 1995), measuring the radiocarbon (^{14}C) content of the CO_2 released from thawed soil profiles definitively tests whether previously-frozen, aged C (depleted in ^{14}C) contributes substantially to release post-thaw.

In addition, quantifying both the rates of C loss from these sources and the C accumulation rates following thaw is required to quantify the consequences of permafrost thaw on ecosystem C balance. It is well established that permafrost thaw in peatlands results in rapid new peat accumulation (Turetsky et al., 2007) and that this accumulation changes with time since thaw (Camill, 1999). Radiometric dating of

peat using ^{210}Pb makes it possible to quantify C accumulation rates for the past ~150 years by assuming a constant supply of atmospheric ^{210}Pb deposited and incorporated in soil (Appleby, 2001; Turetsky et al., 2004). Finally, in terms of determining whether thaw under oxic or anoxic conditions has the greatest impact in terms of changes in global warming potential, any increase in CH_4 flux (Cooper et al., 2017; Turetsky et al., 2007) must also be considered together with the change in C balance.

To determine how the hydrological conditions after permafrost thaw control feedbacks to climate change, we studied the consequences of thaw in peatlands and well-drained fire sites in the sporadic and discontinuous permafrost zones of north-west Canada. We measured fluxes and sources of CO_2, as well as changes in C accumulation rates to quantify the effects on ecosystem C balance, and placed these findings into the context of previously-published research on the rates, and sources, of CH_4 release from the same sites (Cooper et al., 2017). Finally, additional incubations were performed to compare our in situ findings with the type of data that are often used to predict the magnitude of the permafrost feedback (Koven et al., 2015). We conclude that in the ecosystems we studied, oxic conditions following thaw are required for permafrost thaw to represent a strong positive feedback to climate change.

## 2. Materials and methods

2.1. Site selection

The fastest and greatest extent of thaw is expected within the discontinuous and sporadic permafrost zones, where permafrost temperatures are close to 0 °C (Brown and Romanovsky, 2008; Camill, 2005). Therefore, we studied peatlands and well-drained sites in the sporadic permafrost zone in Yukon (2013) and in the extensive discontinuous permafrost zone (Brown et al., 1997) in Northwest Territories, NWT (2014). Research was undertaken at four study sites: a peatland near Teslin (Yukon peatland), a peatland near Yellowknife (NWT peatland), an upland forest near Whitehorse (Yukon well-drained forest), and a forest near Behchoko (NWT well-drained forest). The mean annual air temperature (MAAT, 1981–2010) for the Yukon peatland was −0.6 °C, with monthly averages ranging from −17.1 °C in January to 14.1 °C in July and the mean annual precipitation (MAP) was 346 mm (Environment Canada, 2015). For the Yukon well-drained forest, the MAAT was −1.4 °C, with monthly averages ranging from −18.2 °C in January to 13.9 °C in July, and the MAP was 228 mm. For the NWT sites, the MAAT was −4.3 °C, with monthly averages ranging from −25.6 °C in January to 17.0 °C in July, and the MAP was 289 mm.

The Yukon peatland study site (Fig. 1a) contained an isolated permafrost peat plateau fringed by a thermokarst wetland (approximate size 30 × 40 m) located near MP788 (Alaskan Highway Milepost), approximately 20 km southeast of Teslin in the Yukon Territory (60°05′27.5″N, 132°22′06.4″W). The peat plateau was elevated up to 1.5 m above the surrounding wetland, with electrical resistivity probe measurements suggesting that permafrost thickness was 15–18 m in the higher parts of the plateau (Lewkowicz et al., 2011). The thermokarst wetland was dominated by hydrophilic sedges (Carex rostrata Stokes), which resulted in the accumulation of sedge-derived peat since thaw. The mean active-layer thickness (ALT) in 2013 in the plateau was 49 cm, while thaw depths exceeded 160 cm in the wetland. The plateau collapsed ~55 yr ago and ~50 cm of pure sedge peat had accumulated since then. A layer of tephra identified as White River Ash present near the base of the active layer (~38 cm) in the peat plateau indicates that the minimum age of the organic matter at the top of the current permafrost layer was 1200 yr BP (Clague et al., 1995). The White River tephra layer (1200 yr BP) was observed at a shallower depth (21 cm) in the Margin of the wetland, where peat was more compacted, and in two Wetland centre cores at 55 and at 102 cm. In this site, we investigated the contribution of deep SOC-derived CO_2 using radiocarbon

a. Yukon peatland
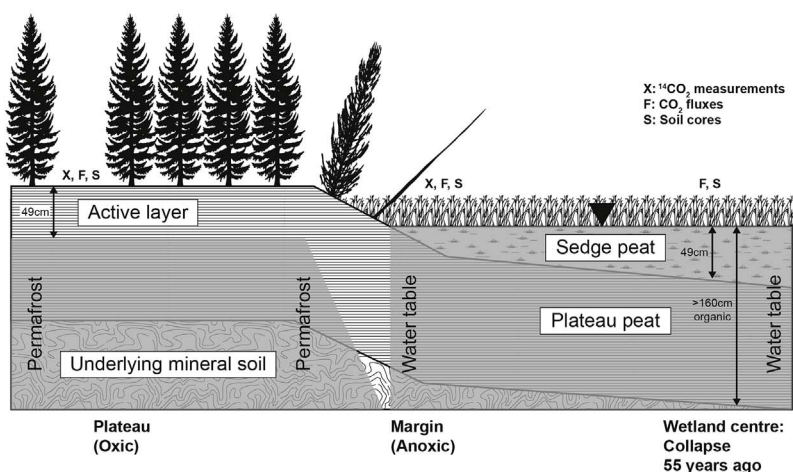
b. NWT peatland
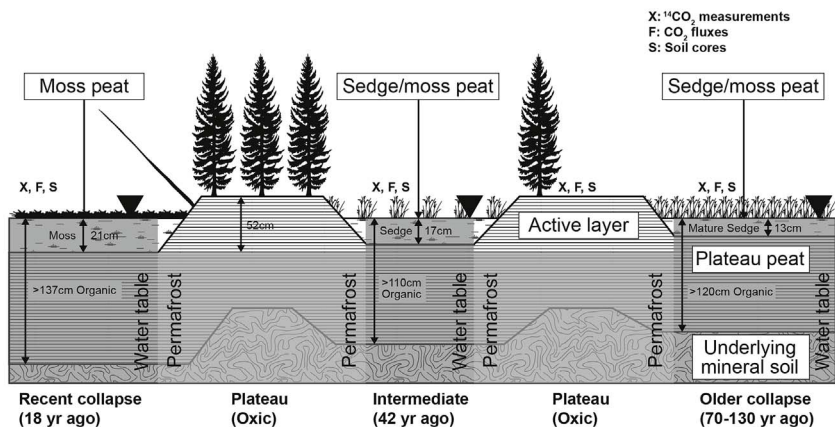
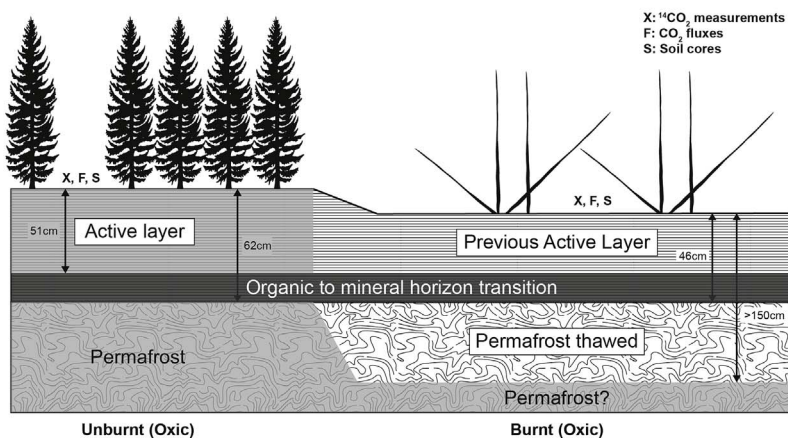**c. NWT well-drained forest**

Fig. 1. Schematic diagram of the site-specific sampling designs. Panel (a) shows the sampling locations in the Yukon peatland site, where the contribution from permafrost SOC to CO_2 flux was investigated at the edge of the wetland (Margin). Radiocarbon CO_2 measurements were also performed in the plateau and CO_2 fluxes were measured in all three locations including the wetland centre. Panel (b) shows the NWT peatland site sampling locations dominated by Moss (recent collapse), Sedge (intermediate collapse age) and Mature sedge (older collapse). The sampling locations for $^{14}CO_2$ were replicated three times in separate *Sphagnum* moss- and sedge-dominated wetlands and in a single mature collapse. The site has a single plateau that contains multiple collapse wetlands and the stratigraphy along the margins is simplified for clarity. Panel (c) represents the sampling locations in the well-drained forests with values for the NWT site and adjacent burnt areas where vegetation was removed by fire and the active layer thickened. The band separating the organic and mineral horizons represents the variable depth of this transition, which influences the contribution of deep SOC respiration to CO_2 flux (see text). The Yukon well-drained forest is also represented by panel (c) taking note of a shallower organic horizon and smaller fire-induced active layer deepening. The soil stratigraphy is not shown to scale; the active layer in the peat plateau and unburnt forests is thinner than the permafrost, whereas the plateau peat in the collapse wetlands is thicker than the post-thaw peat. Values shown are averages (see Table 1).

measurements by sampling in the peatland plateau and at the wetland margin (Fig. 1a), where the greatest rates of previously-frozen C release were expected (Jones et al., 2016).

The NWT peatland study site (Fig. 1b) was a peat plateau thermokarst wetland complex approximately 8 km west of Yellowknife, in the Great Slave Lake region (62°27′25.7″ N, 114°31′59.8″ W). Approximately 65% of the Great Slave Lake region is underlain by thin permafrost exhibiting widespread signs of degradation (Morse et al., 2016). The underlying bedrock constitutes part of the Canadian Shield, consisting of Precambrian granites. At the end of the last glacial maximum, the whole Yellowknife region was submerged by glacial Lake McConnell. During the Holocene, the lake recessed, resulting in permafrost aggradation within lacustrine sediments and peat mound formation in the newly exposed land (Wolfe and Morse, 2016). The site contains an intact peat plateau surrounded by multiple thermokarst wetlands characterized by two distinct vegetation communities: 1) sedge-dominated (*Carex rostrata*) with isolated moss patches, and 2) *Sphagnum* spp moss carpet with little vascular plant cover. A more mature thermokarst wetland was dominated by sedge, with occasional shrubs. The ALT on the plateau in 2014 was 52 cm, while thaw depths in the thermokarst wetlands were around 140 cm, with clay below. Transition depths between post-thaw and plateau peat were shallower (11–23 cm) than in Yukon (Table 1). In the NWT peatland site (Fig. 1b), we contrasted the contribution of permafrost-derived CO_2 release in recent (18 yr ago, moss-dominated), intermediate (42 yr ago, sedge-dominated surface peat) and more mature (70–130 yr ago, mature sedge) collapse wetlands.

The Yukon well-drained forest was an upland site on a hillslope near Whitehorse (61°23′00.1″N, 135°39′34.5″W) which was affected by fire in 1998. We established sampling locations in the burnt forest and an adjacent unburnt area. The ALT was 57 cm in the unburnt area and 61 cm in burnt area. The organic horizon was slightly thicker on average in the unburnt area (47 ± 12 cm) than in the burnt area (43 ± 11 cm), with some areas reaching a depth of 80 cm in the former. The mineral horizon was characterized by brown and grey silty sand containing angular and sub-angular pebbles up to 6 cm in maximum dimension. The effects of fire on the ALT were limited and frequent rock outcrops were encountered above 1 m depth, preventing accurate quantification of the SOC stocks for the top 1 m (maximum depth of soil cores was 56 ± 15 cm, n = 5; note this shallower depth in the SOC stocks quantified for this site in Table 1).

The NWT well-drained forest site (Fig. 1c), adjacent to the Great Slave Lake, was a gently sloping (6–8°) black spruce forest (*Picea mariana*) affected by a large fire in 2008 (62°42′2.3″ N, 116°8′8.8″ W). Vegetation in the unburnt was dominated by feather mosses, predominantly *Hylocomium splendens*, which were removed in the burnt area, where there was evidence of extensive ground scorching and bare ground coverage, with shrub birch (*Betula glandulosa*) and other shrubby species (*Rhododendron groenlandicum* and *Vaccinium vitis-idaea*) beginning to re-establish (Fisher et al., 2016). The mean organic horizon thickness was 62 ± 18 cm in the unburnt area and 46 ± 16 cm in the burnt. The organic horizon sharply transitioned into underlying grey sand (80% sand content) loosely cemented with pore ice. The mean ALT in the study year was 51 cm in the unburnt area and at least 123 cm in the burnt (a conservative value since our maximum measureable depth of 150 cm was exceeded in 18 of 35 measured locations). The active layer had a variable and lower SOC stock (37 kg C m^{-2} down to 1 m) than in peatlands due to a variable and shallower organic horizon (~60 cm) and low C content in the mineral horizon (< 0.5% dry weight). The fire-induced thickening of the active layer increased the C stock available to decompose to at least 55 kg C m^{-2} (to 1 m), with approximately two thirds of the additional C being contained within a previously-frozen organic horizon. In both well-drained sites we performed $^{14}CO_2$ measurements in undisturbed and adjacent burnt areas to investigate permafrost C release (Fig. 1c).

2.2. Soil physical conditions

Thaw depth was recorded with a frost probe. Water-table depth was measured in the collapse wetlands as the height relative to a datum. To set the datum, a 2–3 m long rod was inserted as deep as possible in the wetland and a mark made on it from which the height to the water table was measured. We did not detect the presence of a liquid water-table above the permafrost in the peat plateaus.

Soil temperatures were recorded with thermistors inserted in tubes that were installed in the soils after the core sampling (see below). These tubes were sealed at the bottom and filled with antifreeze. We also used a Rototherm probe (British Rototherm Co. Ltd. Port Talbot, UK) that consisted of a robust 1.3 m long tube of stainless steel (11 mm outer diameter, 7 mm inner diameter) with a sensing tip containing a platinum resistor (100 Ω at 0 °C, 4 wire, Class B, made to IEC 751 Standard; manufacturer's stated tolerance ± 0.3 °C) connected to a hand-held digital thermometer. Soil temperatures are summarized in Fig. S1.

2.3. Heterotrophic CO_2 respiration fluxes

Heterotrophic respiration fluxes were measured generally weekly to biweekly using the static chamber method (Livingston et al., 1995). Collars made of PVC (internal diameter 30 cm in collapse wetlands and 16 cm elsewhere) were inserted 35 cm into the soil and vascular vegetation was clipped on the surface. To minimize the autotrophic component (plant and root respiration), the location of the collars was trenched and clipped during the previous summer in the plateaus and well-drained sites by cutting into the soil using a serrated knife. For the thermokarst wetlands, the collars were inserted at the start of the growing season in which fluxes were measured, before any live sedge biomass was produced, and all green shoots were continuously removed during the season. Three to five replicate collars were installed at each investigated location. Concentrations of CO_2 in the plateaus and well-drained sites were measured for 2 min using an EGM-4 Infrared Gas Analyser with a CPY-4 chamber (PP Systems) covered to ensure dark conditions. In the collapse wetlands, PVC chambers (15–35 cm high) were sealed to the collars using rubber tubes, with fluxes measured for 3 min during which concentrations were recorded at 10 s intervals. The slopes of the linear regression of CO_2 concentrations and time were used as flux rates and yielded R^2 values > 0.95.

2.4. $^{14}CO_2$ sample collection and analysis

We estimated the contribution of CO_2 derived from previously-frozen C by measuring the ^{14}C content of CO_2 from two collar treatments (Fig. S2) made from PVC pipe with an internal diameter of 30 cm (collapse wetlands) and 16 cm (all other sites). The first collar type was a full-profile collar inserted 35 cm into the soil, except in the Yukon plateau, where frozen ground at time of installation limited the depth of insertion to 30 cm. For the second collar type, 35 cm long cores were extracted (30 cm in Yukon plateau) using a serrated knife, transferred into cylinders with sealed bottoms to exclude any CO_2 contributions from depth (near-surface collars) and re-inserted (Cooper et al., 2017). Any vascular vegetation regrowing at the surface of the collars was clipped, but the moss surface was left intact, except in the moss-dominated NWT collapse wetland, where the capitulum of *Sphagnum* (1–2 cm) was removed to minimize autotrophic respiration. In the collapse wetlands, the near-surface collars contained both post-thaw and plateau peat as the transition depth between both peat types was shallower than 35 cm in the Margin in Yukon and in the NWT wetlands (Table 1). Probes made of stainless steel tube (6 mm outer diameter, 4 mm inner diameter, Swagelok) perforated at the base and covered with a waterproof but gas-permeable membrane (Accurel Membrana GmbH) were inserted to collect CO_2 gas at the same depth as the base of the collars. The ^{14}C content of the CO_2 collected by the probes, and the

Table 1
Summary of physical and soil core properties in the investigated sites. Values show mean ± SD (n) or range when n = 2.

Site-Oxic/Anoxic	Depth (cm)				Carbon stock (kg C m^{-2})[a]				Age of collapse (yr ago)[b]		C accumulation rates (g C m^{-2} yr^{-1})		
	Organic horizon	Active layer	Post- to pre-thaw peat	White River Ash	Active layer	Permafrost to 1 m depth	Surface to 1 m depth		^{210}Pb dating	^{14}C dating	^{210}Pb - 100 yr period	1200 yr BP - White River Ash
Yukon Plateau-Oxic	> 115	49 ± 4(5)	NA	38 ± 2(3)	22.9 ± 4.4(3)	33.1 ± 7.1(3)	56.1 ± 11.5(3)	NA	NA	35.7 ± 2.8(3)	12.86 ± 1.67(3)
Yukon Margin-Anox.	> 140	NA	NA	21 ± 5(3)	NA	NA	121.1–134.2 (2)	NA	NA	64.2 ± 31.5(4)	9.90 ± 3.34(3)[f]
Yukon Wetland-Anox.	> 160	NA	49 ± 22(5)	55–102(2)	NA	NA	57.4 ± 18.3(5)	55 ± 28(5)	57 ± 32(5)	149.9 ± 55.2(5)	22.39–31.05(2)
NWT Plateau-Oxic	> 110	52 ± 2(5)	NA	NA	26.0 ± 5.1(5)	33.1 ± 5.7(5)	59.1 ± 9.2(5)	NA	NA	30.2 ± 4.8(5)	NA
NWT Moss-Anoxic	137–176	NA	21 ± 2(5)	NA	NA	NA	53.6 ± 16.3(5)	18 ± 3(5)	21 ± 1(3)	81.4 ± 24.2(5)	NA
NWT Sedge-Anoxic	110–145	NA	17 ± 5(5)	NA	NA	NA	55.5 ± 12.9(5)	42 ± 14(5)	51 ± 57(3)	63.1 ± 15.3(5)	NA
NWT Mature-Anoxic	120–130	NA	13 ± 2(5)	NA	NA	NA	49.9 ± 13.8(5)	68 ± 10(5)	132 ± 27(3)	50.6 ± 6.9(5)	NA
Yukon Unburnt-Oxic	45 ± 8(30)	57 ± 7(30)	NA	NA	22.6 ± 4.1(3)	23.2 ± 2.2(3)[d]	45.7 ± 5.3(3)[d]	NA	NA	40.0 ± 17.4(5)	NA
Yukon Burnt-Oxic	43 ± 11(23)	61 ± 13(30)	NA	NA	NA	NA	23.1 ± 7.7(5)[d]	NA	NA	29.2 ± 1.9(5)[e]	NA
NWT Unburnt-Oxic	62 ± 18(35)	51 ± 9(35)	NA	NA	37.2 ± 13.3(5)	18.8 ± 9.7(5)	56.1 ± 22.0(5)	NA	NA	57.9 ± 17.8(4)	NA
NWT Burnt-Oxic	46 ± 16(35)	123 ± 32 (35)[c]	NA	NA	NA	NA	52.4 ± 12.4(5)	NA	NA	26.8 ± 7.4(5)[e]	NA

[a] Permafrost to 1 m depth refers to frozen soil until 1 m deep and Surface to 1 m depth includes both active layer and permafrost down to 1 meter.

[b] Age is given in years since time of sampling (2013 for Yukon and 2014 for NWT).

[c] The mean active layer thickness represents an underestimate as 18 of 35 surveyed locations were > 150 cm, our deepest measurable thaw depth in late summer.

[d] In the unburnt, only 3 cores reached between 78 and 100 cm (shown data). In the burnt, the maximum depth was 56 ± 15 cm, n = 5 (shown data).

[e] The C accumulation in the burnt sites is used to estimate how much organic matter was burnt in the top soil profile (Supplementary material).

[f] C accumulation rates in the margin were not significantly different to those in the plateau (P = .25, two-sample independent t-test).

119

[14]C contents of the soil organic matter (see soil sampling in Section 2.5), were used to calculate the contribution of deep SOC respiration. Tygon tubing with CPC couplings at the surface end of probe prevented atmospheric air entering the probe. These probes were connected to molecular sieves cartridges with Type 13X Zeolite for passive CO_2 collection (Garnett et al., 2009). Three replicates of each collar type and probe were sampled in each location.

To collect CO_2 from collars for ^{14}C analysis, PVC chambers were placed on top of the collars and CO_2 left to accumulate until concentrations exceeded 800 ppm. To reduce the atmospheric CO_2 component in the headspace, the volume was then circulated between the chamber and a soda lime trap using a closed-loop configuration, reducing CO_2 concentrations to levels around 200 ppm (the values attained depended on the balance between the rates of production and removal). Subsequently, CO_2 concentrations were left to increase again and a molecular sieve (Type 13X Zeolite) was connected to the chamber to collect CO_2 by passive diffusion (Garnett et al., 2009; Garnett and Hardie, 2009). The sieve was connected to the chamber for about a week and then disconnected. To obtain a representative ^{14}C signature of the late growing season this procedure was performed twice by connecting the same sieve to the same sampling location at the end of July/ early August and then again at the end of August/early September. Sieves were sent to the NERC Radiocarbon Facility (UK) for graphitization and ^{14}C analysis. Following convention, radiocarbon results were expressed as conventional radiocarbon years before present (BP; where 0 BP = AD 1950) and %modern (Stuiver and Polach, 1977). The maximum analytical uncertainty of our measurements was 0.5 % modern.

2.5. Soil sampling and soil organic carbon quantification

Five soil cores (replicates) to 1 m depth were sampled at each study location, except in the burnt forest in Yukon where rocks were encountered at depths above 1 m. The upper part of the core was obtained using aluminium monolith tins (40 × 10 × 4 cm) that minimized disturbance and compaction of the soil profile. Frozen ground was sampled using a CRREL powerhead corer (Rand and Mellor, 1985) to recover soil sections of 5 cm diameter and variable length (usually 10–15 cm), which were wrapped in sealed plastic bags and placed in PVC tubes cut in halves for secure transportation. In the collapse wetlands we used the same monolith tins, as well as a Russian corer to sample deeper soil, which was placed on half-cut PVC tube, wrapped with plastic and secured with rigid plastic on top. Samples were kept frozen in Canada until they were shipped to the UK for sectioning and analysis. Soil cores were cut into sections of known volume and analysed for bulk density and carbon content. The upper part of the core (usually down to 40 cm depth) was cut at 1 cm depth increments for lead dating analyses (see dating). Deeper parts of the core were cut usually into 10 cm sections or when changes between the organic and mineral horizons were observed. Samples were freeze dried and weighted to calculate bulk density, and manually ground prior to carbon content determination. C and N content was determined using an organic elemental analyser (Flash 2000, ThermoScientific). SOC stocks were quantified by interpolating the measured bulk density and C content over the length of the sampled intervals.

2.6. Soil dating: [14]C and [210]Pb

A stratigraphic transition between deeper, plateau peat (peat aggraded under permafrost conditions and typically identified by the presence of lichens and woody remnants (Robinson and Moore, 2000; Zoltai, 1995)) and shallower, post-thaw peat (associated with the change in vegetation community after thaw (Camill, 1999; Turetsky et al., 2000)) was clear in all cores from the collapse wetlands. We used this transition in the wetland cores to date the time of plateau collapse using ^{210}Pb dating in all sampled cores and ^{14}C dating of plant

macrofossils identified in selected cores. We used the tephra layer from the eastern lobe of the White River volcanic eruption deposited ∼1200 yr BP (Clague et al., 1995; Robinson, 2001; Robinson and Moore, 2000) as a chronostratigraphic marker in the Yukon peatland site. Additional soil was ^{14}C dated in deeper sections, at depths similar to the base of the probes collecting [14]CO_2 and also to verify that the tephra layer corresponded to the White River Ash (Table S1). Radiocarbon ages were calibrated using CaliBomb (IntCal 13 calibration data set, Levin Bomb curve extension), taking the mean value of the highest probability calibrated BP range (1 sigma). [210]Pb dating was used to quantify recent (< 100 years) carbon accumulation rates following a procedure adapted for organic samples. [210]Pb activity was quantified by alpha spectrometry, which measures [210]Po decay as a proxy for [210]Pb. A [209]Po spike (1 ml) was added at the start of the preparation as a chemical yield tracer. Freeze-dried and ground samples (∼0.5 g dry weight) were prepared by acid digestion, using concentrated HNO_3, 30% H_2O_2 and 6 M HCl (1:2:1), sequentially added and dried. The supernatant from centrifuged samples was decanted into a 0.5 M HCl solution with 0.2 g ascorbic acid. Po was then electroplated onto silver planchets suspended in the solution for a minimum of 24 h [210]Po decay was measured in the University of Exeter Radiometry Laboratory using an Ortec Octête Plus Integrated Alpha-Spectroscopy System with the software Maestro-32 for a minimum of 24 h until, if possible, a minimum count of 400 was achieved. Such counts were not achieved in the deepest dated samples, with activity approaching near zero. Age-depth profiles were calculated using a Constant Rate of Supply (CRS) model (Appleby, 2001). Though we quantified C accumulation rates for the period since time of thaw, we also present C accumulation rates over a 100 yr period (Table 1) to compare with other studies reporting around 80–100 g C m^{-2} yr^{-1} in 100 yr time periods in western Canada (Turetsky et al., 2007, 2000). We also used the ^{210}Pb chronologies in the well-drained forest sites to estimate the fraction of soil removed by combustion during the fire events (Supplementary materials – Comparison between respired permafrost C losses and combustion C losses in well-drained forests).

2.7. Estimates of respired CO_2 from deep SOC sources

Our collar approach compares the ^{14}C content of CO_2 released from two types of collars to determine the contribution of deep SOC respiration to the total flux. In the near-surface collar, the ^{14}C signature of deep soil respiration is physically removed and thus excluded from the CO_2 released, whereas in full profile collars the CO_2 released accounts for the respiration occurring in the entire soil profile thus including soil layers deeper than the base of the near surface collar. Given that the ^{14}C content of SOC decreases with depth and that we inserted the collars to depths that include the bomb ^{14}C peak, we expect CO_2 released from full-profile collars to be depleted in ^{14}C compared to CO_2 released in near-surface collars if there is a quantifiable contribution of respiration from deep SOC sources.

We estimated the contribution of CO_2 derived from sources deeper than the near-surface collars using Equation (1). These sources account for deep active-layer SOC in the undisturbed sites, whereas they also represent CO_2 derived from previously-frozen C in the disturbed sites (burnt areas and collapse wetlands).

$$\text{Deep } CO_2(\%) = \left(\frac{FP^{14}CO_2 - NS^{14}CO_2}{Probe^{14}CO_2 - NS^{14}CO_2} \right) *100 \tag{1}$$

Where Deep CO_2 (%) is the % contribution of CO_2 derived from previously-frozen carbon to total gas efflux, $FP^{14}CO_2$ is the ^{14}C content of the CO_2 collected from the full-profile collars, $NS^{14}CO_2$ is the ^{14}C content of the CO_2 collected from the near-surface collars, and Probe$^{14}CO_2$ is the ^{14}C content of the CO_2 collected from the soil porespace using the probes at the same depth as the base of the near-surface collars (Fig. S2). The condition for a possible quantification of this

contribution from depth is that $FP^{14}CO_2$ is lower than $NS^{14}CO_2$ (lower $FP^{14}CO_2$ than $NS^{14}CO_2$ indicates that sources older than the base of the near-surface collar contribute to CO_2 release). We calculated Deep CO_2 (%) using as end member from depth the $Probe^{14}CO_2$. Additionally, Deep CO_2 (%) was calculated using a range of SOC ages as end members at depth (replacing $Probe^{14}CO_2$ in Equation (1)) to represent previously-frozen C sources in the disturbed sites. We conservatively established that the SOC age at the top of permafrost was 1200 yr BP in the peatlands and 2000 yr BP in the forests based on chronostratigraphical markers, ^{14}C dating of soil and ALT of the sites.

2.8. Estimates of net C balance and net CO_2 equivalents in peatland soils

We calculated the net C balance in the peat plateaus and collapse wetlands soils for the time period since thaw. For this, we subtracted the annual C losses from the annual C gains in the soils for that period. We defined the C gains as the annual C accumulation rates measured for that period using ^{210}Pb and radiocarbon dating. We defined the annual C losses as the seasonal release of CO_2 derived from permafrost C estimated using our $^{14}CO_2$ measurements (Section 2.7). For this, we multiplied the contributions of Deep CO_2 (%) by our seasonal cumulative heterotrophic fluxes (section 2.3) to estimate the annual loss of previously-frozen C. We assume that these estimates of C loss measured in a single year remain the same for all the time period since thaw. The net CO_2 equivalents balance was estimated for the same period from the difference in CH_4 release (converted to CO_2 equivalents using a weight-corrected Global Warming Potential, GWP, of 34 over a 100 yr period (Myhre et al., 2013)) and the CO_2 uptake from C accumulation rates. These calculations refer to soil C balance and not to the ecosystem C balance; plateaus do not include C sequestration from trees which, despite a likely low rate of C accumulation would contribute to make their C and CO_2 equivalents balance slightly more negative.

2.9. Incubations

To compare our field measurements with rates of previously-frozen C release that would have been predicted based on incubations, we carried out an 84-day incubation experiment with peat sampled from the Yukon collapse wetland (section 2.7). To this aim, we quantified, at 5 and 15 °C, aerobic and anaerobic potential production rates of CO_2 and CH_4 from peat collected from four different depths: 1) the top sedge peat between 6 and 23 cm, 2) deeper sedge peat between 30 and 52 cm, 3) thawed plateau permafrost peat between 74 and 104 cm and 4) deeper thawed permafrost between 103 and 143 cm. We incubated three replicates of each depth from separate peat cores for each temperature and oxygen treatment (both oxic and anoxic conditions). Peat was contained in plastic pots. For the anoxic incubations, the peat was submerged with distilled water, placed inside 0.5 L glass kilner jars with sealed air-tight lids and the headspace was flushed with nitrogen gas through tygon tubing that also allowed gas sample collection through CPC couplings shut-off valves. Plastidip was used to further ensure that the kilner jars in the anoxic incubations were air-tight. In the oxic incubations, the peat was maintained at near field capacity by adding distilled water and the samples were placed into 0.5 L plastic jars to measure CO_2 production rates. The amount of peat in each jar varied between 3 and 10 g peat (dry weight), with reduced masses in the sedge peats due to their low bulk density. Production rates of CO_2 and CH_4 were calculated from the change in concentration in the headspace over time, with samples initially collected weekly and then monthly as fluxes declined over an 84 day period. Concentrations were determined using an EGM-4 analyser and Detecto Pak Infrared CH_4 analyser (DP-IR, Heath Consultants Inc) for CO_2 and CH_4, respectively. For the anoxic incubations, gas samples were collected by syringe and injected into a closed loop with a low background of CO_2 and CH_4. The change in concentration in the loop was recorded and the headspace concentration calculated using the loop volume, the injected volume and the

background and final concentrations. For the oxic incubations, concentrations were measured by circulating the headspace through the analysers in a closed loop through a pair of shut-off valves on the lids of the incubation jars. Concentrations at each time were converted to mass of C using the ideal gas law, correcting for temperature. Production rates were standardized to soil C mass for each jar determined at the end of the incubation by drying the soil (dry mass) and determining C and N content as previously described. Based on the total amount of C released over the incubation, we calculated Q_{10} values for each pair of jars (i.e. subsample of a particular depth from each core incubated at 5 and 15 °C). We used these data to correct the rates measured in the incubation to the seasonal soil temperatures measured in the field for each interval depth. We then used bulk density of each depth, previously determined for the soil C stocks quantification (interpolating between the sample depths), to calculate the flux on an area basis and added the flux of all intervals to estimate the total flux. We then estimated the contribution of one or both deep intervals from permafrost sources (layers 3 and 4 above) to the total flux (we conservatively make this distinction because it could be possible that part of the shallower thawed plateau permafrost peat layer between 74 and 104 cm was not permafrost but part of the active layer before thaw). The calculated contributions of permafrost C sources from the incubation data were used for comparison with the in situ measurements but were not used for estimating net C balance.

2.10. Statistical analysis

Statistical analyses were carried out using SPSS (Version 22, SPSS Science) and data were checked for suitability for parametric analysis. Three-way, repeated measures analysis of variance was carried out to examine differences in $^{14}CO_2$ released between collar type (within subject factor) among ecosystem type and region (between-subject factors) and repeated measures ANOVAs were also used to evaluate differences in heterotrophic CO_2 flux between sites over time. Paired t-tests were used to evaluate if the mean differences in $^{14}CO_2$ released between type of collar differed from zero in oxic undisturbed (plateaus and unburnt forests) and anoxic (collapse wetlands) sites. Two-sample independent t-tests were performed to evaluate if the mean rates of C accumulation and CO_2 flux differed between undisturbed and disturbed locations within a site on individual measurement dates.

3. Results

3.1. CO_2 fluxes

In the peatlands, we observed differences in rates of CO_2 release from collapse wetlands and undisturbed plateaus, but these were not consistent between sites likely due to the contrasting seasonal moisture conditions between years/sites. In Yukon, CO_2 fluxes from heterotrophic respiration were greater in the plateau than in the wetland (Fig. 2a), where the water-table remained high and stable, within 5 cm of the soil surface throughout the 2013 growing season (Fig. 2c). We estimated a CO_2 release of 168 g C m^{-2} in the plateau and up to 90 g C m^{-2} in the wetland during the growing season (70 days, measurements until September). In NWT, an anomalously dry summer in 2014, with 20 mm of rain in June and July, representing just 30% of the long-term average rainfall for these months, resulted in the water-table in the wetlands falling to a mean depth of 25 cm. The prolonged drying boosted aerobic respiration in the near-surface peat in the wetlands, and limited respiration in the plateau (Fig. 2b and c). Measurements on the same day before and immediately after rain (Julian day 229) provide evidence for moisture stress in the plateau, with the flux increased by a factor of over 3 upon rewetting after the prolonged drying (data not shown). Due to the dry conditions, CO_2 release over the growing season in NWT was significantly lower in the plateau (78 g C m^{-2}) than in the moss and young sedge wetlands (115 and 148 g C m^{-2}, P < .05).
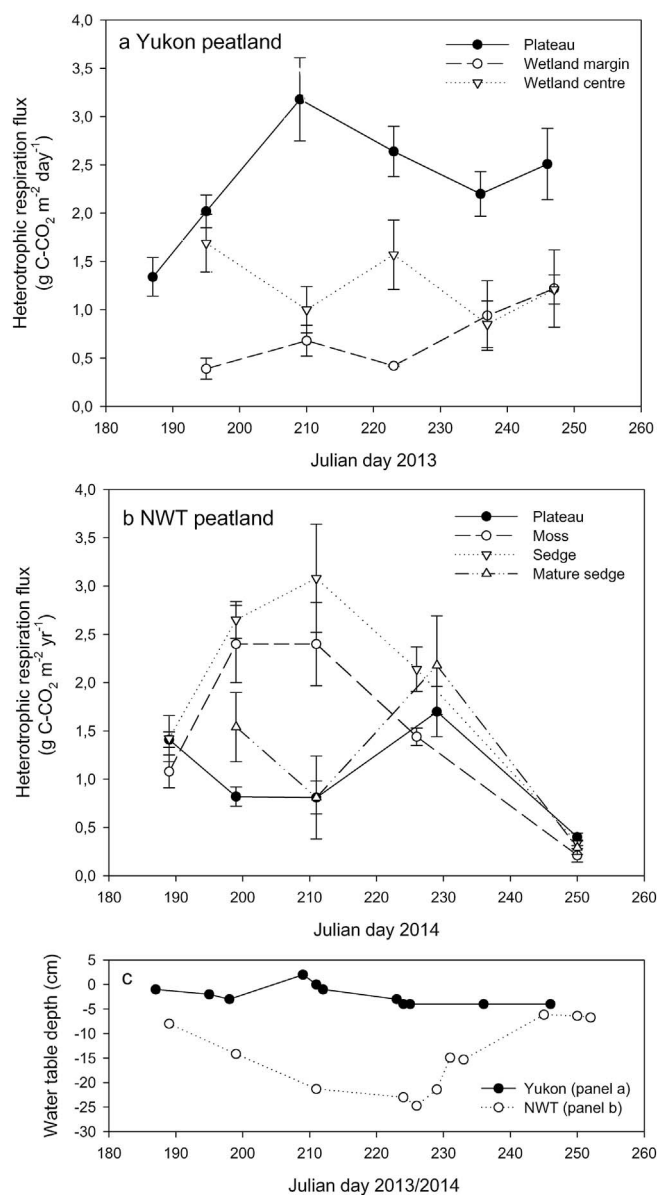
Fig. 2. Growing season CO_2 fluxes from heterotrophic respiration in peatland plateaus and collapse wetland locations. Fluxes here refer to measurements from full profile collars. Panel (a) shows measurements in Yukon and panel (b) in NWT peatland sites (mean ± s.e.m.; n = 5 in plateaus and n = 3 in collapse wetland locations for measurements at each time point). The Moss, Sedge and Mature sedge locations in panel (b) correspond to the recent, intermediate and mature collapse wetlands shown in Fig. 1b. Panel (c) shows the contrasting water table between Yukon (high and stable) and the NWT (severe summer drought). Water table in Yukon was at a single location, but data from NWT are based on three moss and three sedge wetlands. Error bars were too small to be shown clearly on the figure (s.e.m. = 1.4 cm, n = 6).

The seasonal flux dynamics in the mature sedge wetland were similar to the plateau with a CO_2 release over the growing season of 84 g C m^{-2}. This could be related to the greater proportion of peat above the water table in the mature sedge site associated with a more advanced developmental stage of peat accretion following thaw. Overall, the differences in CO_2 flux between plateaus and collapse wetlands were controlled by the contrasting seasonal moisture regime (Fig. 2).

In the well-drained forest areas, despite the removal of live trees and loss of recent C inputs in the burnt sites, heterotrophic respiration fluxes were never significantly lower in the burnt locations than the unburnt locations (Fig. 3). Fluxes did not differ significantly between the burnt and unburnt forest in Yukon (Fig. 3a) resulting in similar cumulative growing season CO_2 release (70 days) in both areas (118 g C m^{-2} in the
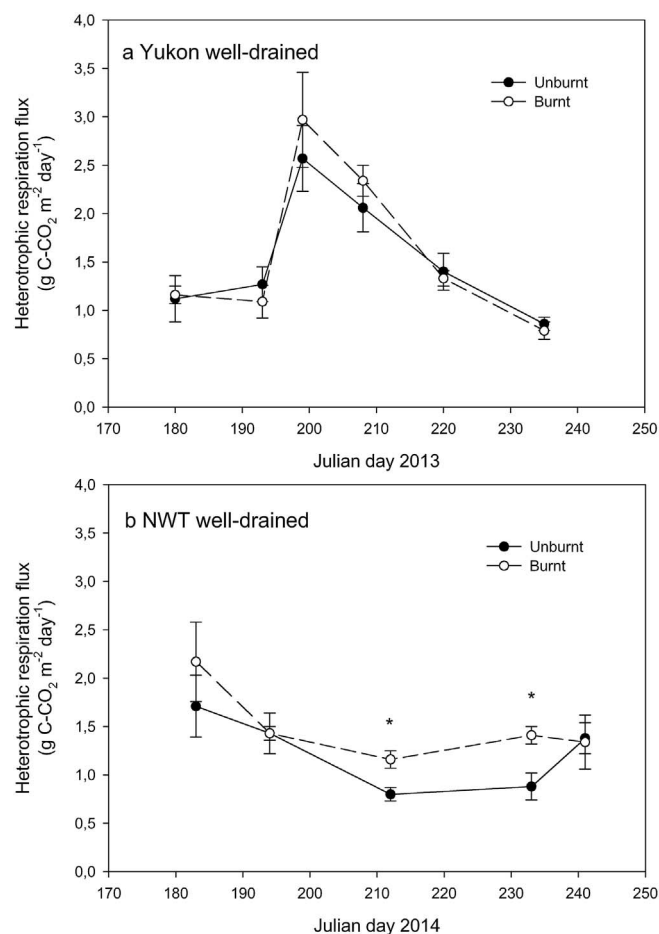

Fig. 3. Growing season CO_2 fluxes from heterotrophic respiration in burnt and unburnt well-drained sites. Panel (a) shows measurements in Yukon and panel (b) in NWT site (mean ± s.e.m.; n = 5 for measurements at each time point). Statistically significant differences in flux between the burnt and unburnt areas for each measurement date are indicated by * (two-sample independent t-test, P < .05).

burnt and 115 g C m^{-2} in the unburnt, P = .79). Fluxes were occasionally significantly greater during mid-season measurements in the burnt area at the NWT site (P < .05), resulting in a slightly higher (although not significant, P = .30) growing season release in the burnt (101 g C m^{-2}) than the unburnt (86 g C m^{-2}) area (Fig. 3b).

3.2. $^{14}CO_2$ and sources contributing to CO_2 flux in oxic and anoxic soils

The contribution of deep C to the surface CO_2 flux depended more on whether the soils were well-drained/oxic or inundated/anoxic than on the amount of SOC available for microbial decomposition (Fig. 4, Table 1, Table S3). This is reflected by the lower radiocarbon contents of CO_2 released from full profile collars (FP$^{14}CO_2$) than from near surface collars (NS$^{14}CO_2$) in the oxic soils (forests and peat plateaus) but not in the anoxic soils (collapse wetlands). Across the four oxic undisturbed sites investigated (both unburnt forests and both peat plateaus), the FP$^{14}CO_2$ was significantly lower compared to NS$^{14}CO_2$ (P = .033). No significant differences in the ^{14}C of CO_2 were observed between ecosystem types (P = .110; unburnt forests and peatland plateaus) or between the two study regions (P = .281; Yukon and NWT) and there were no significant interactions between collar type and ecosystem type (P = .816) or region (P = .772). The ages of CO_2 collected at depth (Probe$^{14}CO_2$) ranged from modern to 690 yr BP in these undisturbed soils. The mean contribution of CO_2 from below the depth of the collars using Probe$^{14}CO_2$ varied between 10.9 and 24.8% (Table S3). In addition, due to the within site variability in the Probe$^{14}CO_2$
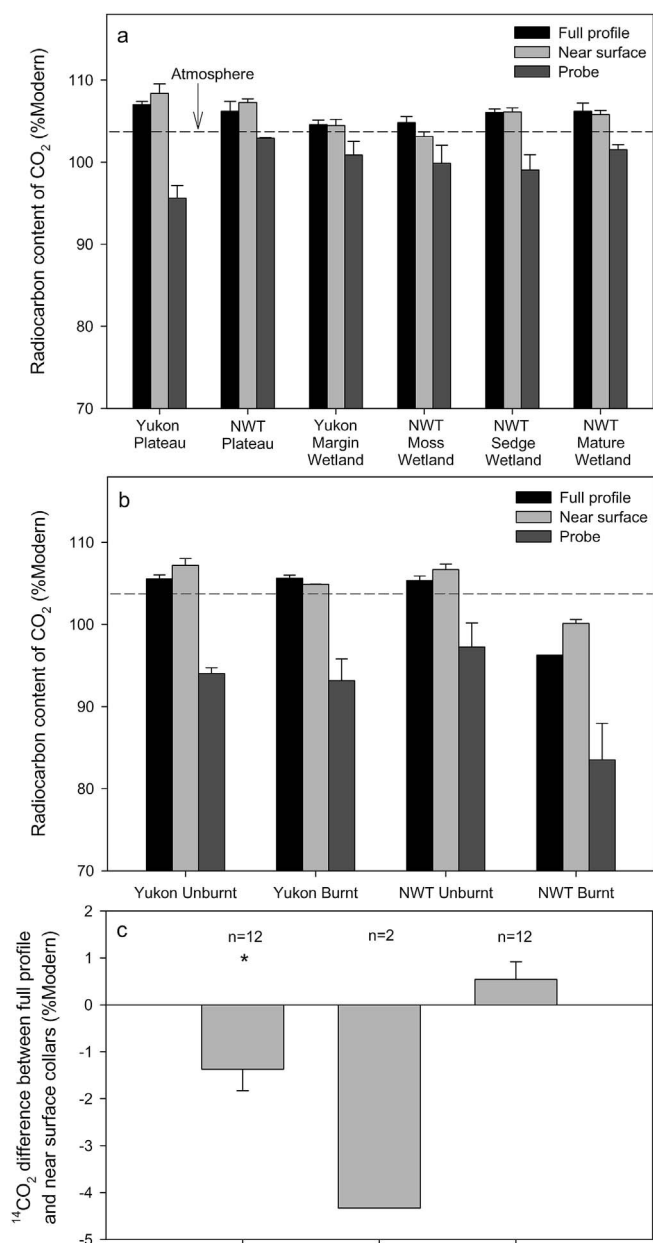
Fig. 4. Mean ^{14}C content of CO_2 collected from full-profile collars, near-surface collars and the probes located at 35 cm depth. Panel (a) contrasts the undisturbed plateaus and the collapse wetlands in the Yukon and NWT peatland sites. Panel (b) compares the undisturbed (unburnt) and burnt forest in the Yukon and NWT well-drained sites. Error bars represent ± s.e.m. (n = 3 for each site and type of sample except n = 2 in the probe at the NWT plateau with values of 102.86 and 102.98 %modern, and in the full-profile collars at the burnt area in the NWT site, with values of 102.75 and 89.79 % modern). The dashed line indicates the average estimated ^{14}C content of the atmosphere in the sampling years. No statistically significant differences between $FP^{14}CO_2$ and $NS^{14}CO_2$ were found within a given site (Supplementary Materials – Radiocarbon content of CO_2 in peatlands). Panel (c) shows the mean difference in $^{14}CO_2$ between paired full-profile and near-surface collars ($FP^{14}CO_2$ - $NS^{14}CO_2$). Error bars indicate ± s.e.m. (n = 12 for both undisturbed sites and wetlands; no error bars shown in the oxic disturbed as n = 2 in the burnt NWT site). Negative values represent depleted $^{14}CO_2$ in full-profile compared to near-surface collars and thus a contribution from deep sources to the flux. The CO_2 released from full-profile collars was depleted in ^{14}C relative to near-surface collars in the undisturbed oxic locations and this difference increased on average in the NWT burnt site. The $^{14}CO_2$ from full-profile collars was not lower than near-surface collars in the wetlands. This indicates measurable contributions to the CO_2 flux of SOC at depth in the oxic soils but not in the anoxic soils. The asterisk symbol indicates significant deviation from zero in the difference between collars (P < .05), but with no statistical analysis for the NWT burnt site (n = 2).

among sites, we also carried out a sensitivity analysis to calculate the mean contribution of CO_2 derived from SOC sources deeper than the base of the collars, by varying the age of SOC at depth (Supplementary materials - Sensitivity analysis and calculation of potential contribution or previously-frozen C, Fig. S3). The results from the undisturbed sites, do not mean that permafrost C (i.e. permanently frozen) was contributing to surface fluxes, but rather demonstrate a measurable contribution from layers below the depth of the near-surface collars (35 cm) to fluxes measured from the full-profile collars in these undisturbed oxic soils (i.e. organic matter decomposing towards the base of the ~ 50 cm deep active layer was contributing to the surface fluxes).

In the NWT burnt site, the ^{14}C content of respired CO_2 indicated that previously-frozen C contributed substantially to the CO_2 flux. In contrast to the unburnt forest, the $FP^{14}CO_2$ was lower than that of the current atmosphere (Levin et al., 2013) indicating older CO_2 release (Fig. 4b). This, together with the fact that fluxes between the unburnt and burnt site were similar and occasionally greater in the burnt area (Fig. 3b), indicates that greater amounts of old C were being released in the burnt in comparison to the unburnt area. In one plot in the NWT burnt area (location 3, Table S2), the Deep CO_2 (%) was estimated to contribute to 52.1% of the flux using the Probe$^{14}CO_2$ (near-surface collar: 100.63 %modern; full-profile collar: 89.79 %modern; probe: 79.81 %modern). A similar conclusion was reached using the age of the SOM itself; organic matter in the burnt area at 35 cm depth was > 2000 yr BP (Table S1) and given that about 15 cm of soil were removed by fire and the ALT was around 50 cm in the unburnt area (Table 1), we consider that the age of the organic matter at the top of the permafrost was at least 2000 yr BP. Using this conservative SOC age, we estimate 47.8% of the surface flux was derived from previously-frozen SOC in that location in the NWT burnt forest. When combined with the heterotrophic flux data, this represents a maximum CO_2 release to the atmosphere of 48 g C m^{-2} during summer derived from permafrost SOC. In contrast, in the Yukon burnt site, permafrost SOC did not make a detectable contribution to surface CO_2 flux (estimates < 0%, Table S3).

In the collapse wetlands, the age of the CO_2 at depth was generally modern and up to 370 yr BP. The $FP^{14}CO_2$ did not differ significantly to that from $NS^{14}CO_2$ (P = .191) in the collapse wetlands (Fig. 4a, wetlands). This indicates that the contribution from respiration at depth, if existing, is on average below detection with our approach. We were previously able to detect a significant contribution (~8.4%, n = 9) of previously-frozen C to CH_4 fluxes in our Yukon study site. With the slightly greater statistical power in the current study of CO_2 fluxes, and given we detected significant contributions of deep soil layers in the undisturbed sites, had there been substantial contributions of deep C to our surface CO_2 fluxes in the collapse wetlands, then our collar method would have been able to detect them.

In summary, the measurable contribution from respired SOC at depth in the oxic ecosystems (plateaus, unburnt forests and NWT burnt site, with the exception of the Yukon burnt forest) contrasted to the undetectable release from deep layers in the anoxic soils of the collapse wetlands (Fig. 4c, Table S3). This was despite much less SOC being available below the depth of the near-surface collars in the oxic ecosystems.

3.3. Comparison with potential decomposition rates from laboratory incubations

We used the potential production rates of CO_2 measured in the incubation experiment to calculate the expected contribution of previously-frozen C to in situ fluxes and compared these estimates with our field measurements from the Yukon wetland. Potential production rates of CO_2 under anoxic conditions declined substantially with peat depth (Fig. S4, see also Figs. S5–S6). These flux estimates and the contribution of each layer using the anoxic cumulative CO_2 release over 84 days are shown in Fig. 5. Our estimates indicate a cumulative C release as CO_2
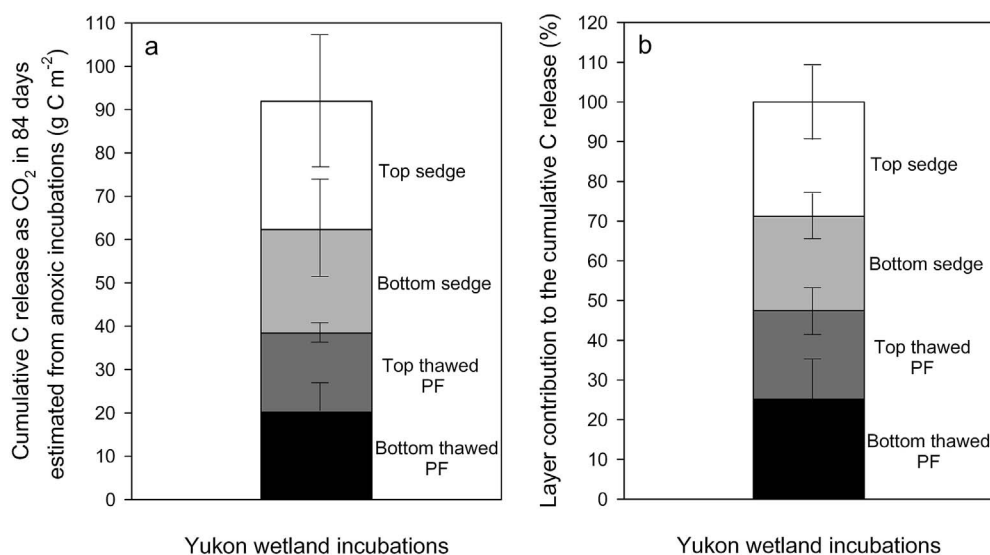
Fig. 5. Incubation-based estimates of rates of C release as CO_2 and contribution of the different peat layers in the Yukon wetland. These estimates are calculated from potential CO_2 production rates in the anoxic incubations at 5 and 15 °C. Panel (a) shows the total mean and layer mean cumulative C release as CO_2 over 84 days of incubation expressed as g C m^{-2} during that period. Panel (b) shows the contribution expressed as percentage obtained from data in panel (a). Error bars represent ± s.e.m. (n = 3). The layers selected are 1) the top sedge between 6 and 23 cm, 2) deeper sedge between 30 and 52 cm, 3) thawed plateau permafrost (PF) peat between 74 and 104 cm and 4) deeper thawed PF between 103 and 143 cm. Measured potential production rates (Figs. S4–S6) and additional estimates of these contributions (Table S4) are shown in the Supplementary Materials – Estimates of contribution from permafrost SOC sources to CO_2 flux in Yukon wetland using incubations.

ranging between 68 and 130 g C m^{-2} over this period with previously-frozen layers contributing between 19 and 67% when both deep layers were considered to have been permafrost (mean of 47% for all three cores), or between 9 and 42% when only the deep layer is considered permafrost (mean of 25% for all three cores). These percentages would on average increase further or remain very similar if, instead of the cumulative data, the initial or final rates of respiration were used to estimate the contribution of the previously-frozen layers, and using a constant Q_{10} value of 2, rather than Q_{10}s calculated for individual pairs of samples, also has very little effect on this calculation (Supplementary materials – Estimates of contribution from permafrost SOC sources to CO_2 flux in Yukon wetland using incubations, Table S4). Even assuming that the top 25 cm of peat was oxic (which is not really representative of the conditions in the Yukon wetland, where the water table remained within 5 cm of the soil surface) we would expect previously-frozen SOC to contribute on average between 12 and 21% of the flux from the wetland. In addition, our incubations only accounted for permafrost down to ~140 cm depth and hence, including the deeper layers of peat would further increase the estimation of the proportional contribution of previously-frozen C to the fluxes post-thaw. These potential contributions from incubations contrast strongly with our in situ $^{14}CO_2$ flux measurements, which did not detect a contribution of previously-frozen C.

3.4. Peatland C balance and global warming potential upon permafrost disturbance

In the peatlands, ^{210}Pb chronologies reveal a rapid increase in the rate of new peat accumulation post-thaw relative to the slow accumulation of the older plateau peat (Fig. S7). We used these age-depth chronologies and the ages of collapse from both ^{210}Pb and ^{14}C dating to contrast the C accumulation rates in the plateaus and the wetlands for the same time period since thaw. Since plateau collapse, peat accumulation rates in the wetlands equate to 1.4 to 6 times those in the plateaus; the greatest rates are in the Yukon collapse site, with mean values > 250 g C m^{-2} yr^{-1} (Fig. 6). The accumulation rate of post-thaw peat decreased with the age of collapse in the NWT sites from 154 to 46 g C m^{-2} yr^{-1} on average (Moss > Sedge > Mature sedge), with surface peat becoming denser through vegetation succession after thaw (Fig. S8). However, the rate of C accumulation post-thaw was more strongly related to the depth of collapse, as indicated by the depth of the plateau peat below the surface (Fig. 7a), rather than to the age of collapse (Fig. 7b). Given that we could not detect a contribution of previously-frozen C to the surface fluxes and that the we observed

enhanced peat accumulation in the collapse wetlands, our C balance calculations result in increased rates of C sequestration in the wetland soils as a result of permafrost thaw in these ecosystems, especially in Yukon (Fig. 8a).

We also considered the implications for changes in global warming potential. Previous measurements of CH_4 release during the growing season in these wetland sites amount to a substantial 21 g CH_4 m^{-2} yr^{-1} in Yukon and up to 3 g CH_4 m^{-2} yr^{-1} in the NWT, the latter value being potential much lower than in a regular year due to drought conditions during 2014 (Cooper et al., 2017). Despite the large CH_4 release in Yukon, the enhanced C sequestration after thermokarst subsidence was estimated to outweigh this in terms of net warming potential in CO_2 equivalents, hence maintaining a net cooling effect on average. However, there was large variability due to within-site spatial differences in surface peat accumulation post-thaw and given that we only have a single year of CH_4 flux measurements this conclusion remains uncertain (Fig. 8b). The enhanced cooling effect relative to the plateau was more apparent in the recent collapse in the NWT, but again this may be due to the low CH_4 release in the study year. The difference in net balance of CO_2 equivalents between the wetlands and the plateau declined from moss to mature sedge, as C accumulation rates declined, suggesting reduced cooling potential with peatland successional at least up to 100 yr post-thaw (Fig. 8b).

The analysis discussed above, especially the unusual drought in the NWT, demonstrates the challenge of linking single year gas flux measurements with multi-year C accumulation data. Reflecting on this, we also considered what the CO_2 equivalents balance may have been in the NWT in a non-drought year by conservatively investigating what the effect would be if, in more average years, the NWT wetlands released 50% of the CH_4 released in the Yukon wetland (Potential No Drought in NWT wetlands in Fig. 8b). Assuming that CH_4 fluxes applied on average to the full period of time since collapse in our studied wetlands (~100 yr ago), this exercise demonstrated the potential for a decrease in the cooling effect relative to the plateau and ultimately the potential for net positive radiative forcing with increasing time since thaw as C accumulation rates decline (Mature sedge).

4. Discussion

4.1. Permafrost C loss in relation to soil oxic conditions post-thaw

In the ecosystems we studied, our results provide direct field evidence that oxic conditions are required for high rates of previously-frozen SOC release, and thus that post-thaw soil moisture is a key
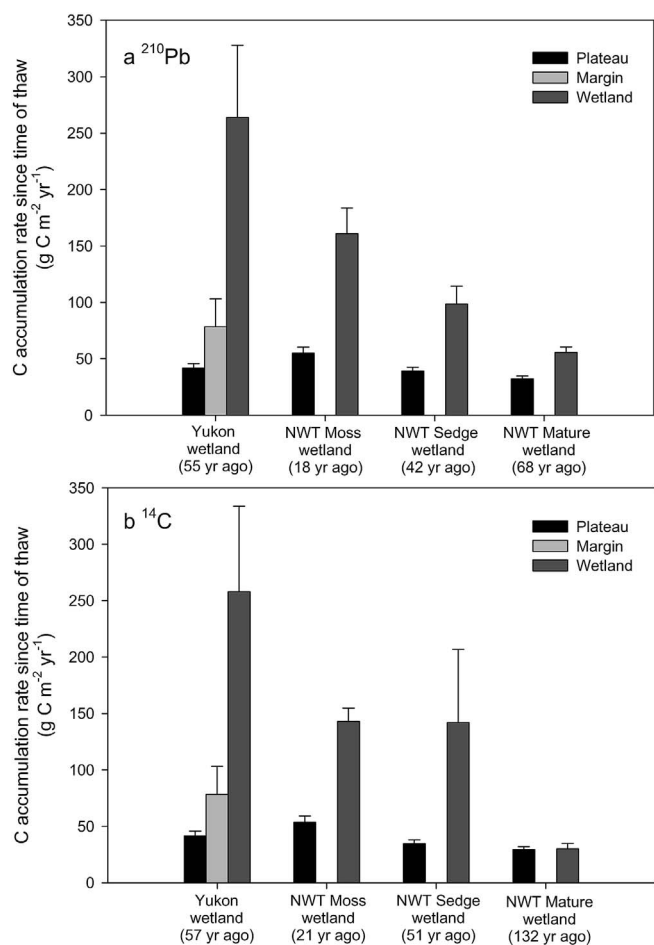
Fig. 6. Mean carbon accumulation rates since time of thaw period in collapse wetlands and peatland plateaus using ^{210}Pb dating (a) and ^{14}C dating (b). Error bars represent ± s.e.m. (for ^{210}Pb dating, n = 3 in Yukon plateau, n = 4 in Yukon margin and n = 5 in Yukon wetland, and plateau, moss, sedge and mature sedge in the NWT site; for ^{14}C dating, n = 3 in Yukon plateau, and moss, sedge and mature sedge in NWT, n = 5 in Yukon wetland and NWT plateau and n = 4 in Yukon margin). The age of thaw (shown in parentheses in the x-axis) was determined by dating the change in stratigraphy between post-thaw and plateau peat using both ^{210}Pb and ^{14}C dating. To compare the rates in collapse wetlands and plateaus over the same period of time (since time of thaw), the transition depth in the wetland cores was dated using ^{210}Pb and ^{14}C to determine the C accumulation and compared to the same timescale on the plateau using the plateau ^{210}Pb chronologies. The time since thaw period for each site and dating method as well as the transition depth between post-thaw and plateau peat is further presented in Table 1.

control of the permafrost C feedback to climate in boreal forests and peatlands (Schädel et al., 2016; Schuur et al., 2015). At sites where aerobic decomposition dominates (i.e. non water-logged sites, except for the Yukon burnt site characterized by shallow organic horizons), we consistently observed lower ^{14}C contents in CO_2 respired from full-profile than in near-surface collars, indicating a measurable contribution from decomposition of deep SOC. While the observation of substantial previously-frozen SOC release was limited to one plot, the fact that measurable contributions from depth were observed in the remaining oxic soils (undisturbed sites) strongly suggests that where thick organic deposits experience aerobic decomposition after thaw, there is the potential for a strong positive feedback to climate change. This agrees with the increased contribution from deeper SOC with active-layer deepening observed in well-drained Alaskan tundra (Schuur et al., 2009).

In contrast, in the collapse wetlands where anaerobic decomposition dominates, the large increase in SOC available for decomposition resulting from the thaw of > 1 m of permafrost peat (thaw more than doubled the C available, Table 1), did not result in a detectable

contribution of old, previously-frozen C being released as CO_2. The lack of a depletion in the radiocarbon content of the CO_2 released from the full profile collars (FP^{14}CO$_2$) relative to that released from the near surface collars (NS^{14}CO$_2$) meant that on average we could not detect a contribution from previously-frozen sources. This was consistent between regions, irrespective of the major differences in water table-depths (wet and stable in Yukon and dry in NWT). While spatial differences may influence the ^{14}CO$_2$ difference between the collar pairs, the pairs of collars were located as close as possible together and we observed a consistent lack of depletion in the FP^{14}CO$_2$ relative to NS^{14}CO$_2$ in all the studied wetlands. Similarly, in a previous study in the same collapse wetlands and study years, we also observed very little previously-frozen C being released as CH$_4$ (< 2 g m^{-2} yr^{-1}, Cooper et al., 2017).

Our findings agree with the observation of limited C release from deep catotelm sources in a non-permafrost peatland exposed to substantial *in situ* experimental warming (Wilson et al., 2016), but contrast strongly with thaw chronosequences measurements that have suggested that 30–50% of peatland C may be lost within decades of thaw in Alaskan sites (Jones et al., 2016; O'Donnell et al., 2012). There are some potential differences in the peat formation processes in these permafrost peatlands. In the Alaskan sites, the permafrost aggraded at the same time as the peat formed (syngenetic permafrost), while in the Yukon site the permafrost may have aggraded after the peat formed (epigenetic permafrost). The rapid incorporation of peat into syngenetic permafrost may explain why peat was on average younger at the base of the active layer in the Alaskan sites than in our sites (~600 yr BP in Alaska and ~1200 yr BP in our study). However, it is unclear if this difference in the incorporation of peat into permafrost between regions results in differences in the quality and lability of the peat that can explain such major discrepancy in rates of previously-frozen C release between studies. Rates of release in Alaska would equate to 3.5 kg C m^{-2} yr^{-1} and fluxes measured in collapse wetlands do not support this rate of release as CO_2 or CH$_4$ (Chasmer et al., 2012; Euskirchen et al., 2014; Johnston et al., 2014; Turetsky et al., 2002; Wickland et al., 2006). Annual C release quantified by eddy covariance in collapse wetlands in Alaska and Canada report ecosystem respiration (including both autotrophic and heterotrophic sources) of < 0.5 kg C m^{-2} annually (Euskirchen et al., 2014; Helbig et al., 2017). Thus, either the major C losses are explained by processes not measured by eddy covariance or ^{14}CO$_2$ fluxes, such as peat erosion or DOC export, or differences in pre-disturbance C stocks between undisturbed plateaus and collapse wetlands may need to be considered carefully when using chronosequences (Jones et al., 2016; O'Donnell et al., 2012).

Finally, it should be noted that the release of relatively large amounts of old C, in the form of CH$_4$, have been observed in thermokarst lakes in Siberia (Walter Anthony et al., 2016). The types of sediments which are exposed in Siberia yedoma regions versus Canadian permafrost peatlands differ strongly, and it is important to note that our current findings should not be extrapolated to conclude that rates of C loss will always be low under anoxic conditions in all sediment types. However, equally, our study emphasises that the results observed in thermokarst lakes can not be applied to predicting fluxes from thawing permafrost peatlands.

4.2. Comparison between respiration and combustion C losses as a result of fire in well-drained forests

Though we mainly focused on forest fires as a means to identify thawed areas and investigate the release of previously-frozen C with active-layer thickening, we also estimated how much C was lost by combustion during a fire. Fire severity was greater in the NWT site than in the Yukon site, as indicated by the greater reduction in organic horizon thickness (Table 1), the ^{210}Pb chronologies (Fig. S9), and the greater age difference in soil organic matter (Table S1) and CO_2 (Table S2) at similar depths in the burnt compared with the unburnt areas. We
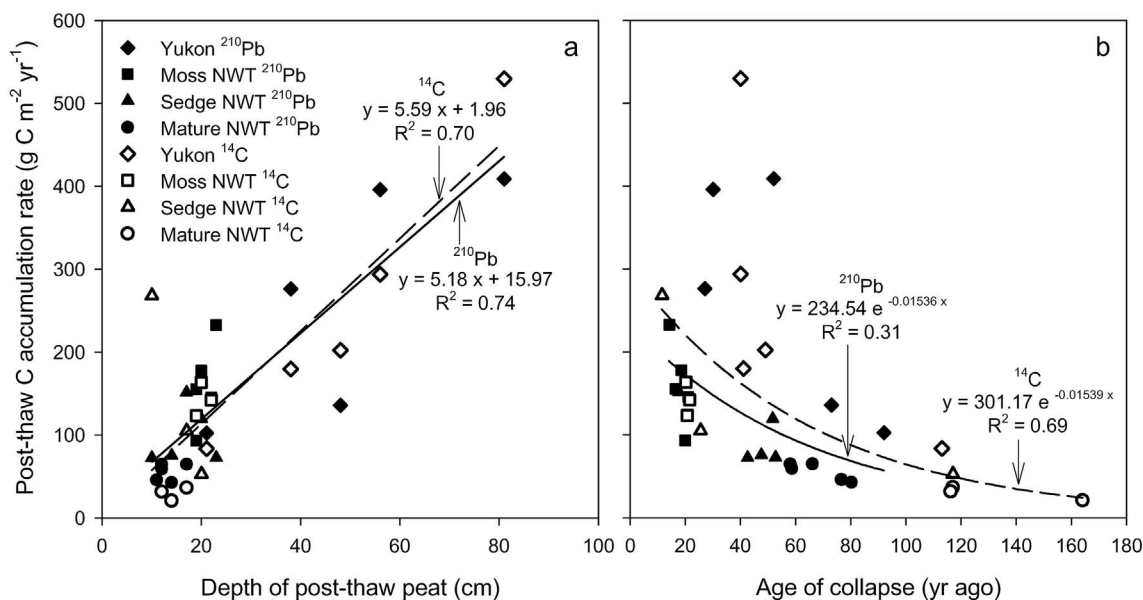
Fig. 7. Relationship between post-thaw C accumulation rates and depth of post-thaw peat (panel a) and age of collapse (panel b) in the collapse wetlands. Each point represents a soil core where the transition depth (visually identified from the clear change in peat stratigraphy between post-thaw and plateau peat) was dated either by ^{210}Pb or ^{14}C. The transition depth is considered as the depth of collapse and potentially relates to ice content in the plateau. A single regression including all data yields $y = 5.37 x + 10.11$ ($R^2 = 0.72$) for panel (a) and $y = 249.11 e^{-0.01457 x}$ ($R^2 = 0.50$) for panel (b). A regular linear model was used to estimate the parameters of the regressions. Adding site as a random factor in a linear mixed effects model showed that site explained no variance in the ^{14}C regression and yielded very similar results estimates in both regressions.

estimated, comparing ^{210}Pb chronologies over the last 100 years between burnt and unburnt cores (Figs. S9 and S10), that fire events removed 5 cm (Yukon) to 16 cm (NWT) of top soil, representing a C stock of 0.84 (Yukon) to 4.52 kg C m^{-2} (NWT), presumably mainly released as CO_2 to the atmosphere. These values agree well with the direct comparison of organic horizons thickness (Table 1). Comparing this recently accumulated C stock released from the surface by combustion to the estimated seasonal release from permafrost SOC by respiration in the NWT site, we note that respired losses from previously-frozen C could potentially equal those from this intense burn after ~90 years. This exercise reflects the importance of fire severity in determining the potential for increased SOC loss, first by removing some of the organic horizon at the surface and subsequently by increasing respiration fluxes through soil warming and the thaw of deeper SOC sources.

In the studied forests, the difference in the contribution of deep C respiration between regions, and the internal variability within the NWT site, likely arises from differences in organic-horizon thickness. The location in which a large amount of previously-frozen C was released in NWT (location 3 in NWT burnt) was characterized by a thick organic horizon and thus substantial amounts of C were exposed following thaw. The Yukon site had a considerably thinner organic horizon with shallow rocks, and the mineral soils had on average very low C contents, potentially explaining why previously-frozen C did not contribute measurably to surface fluxes. Overall, our results indicate that where substantial amounts of previously-frozen C occur, they can contribute an important component of surface fluxes when soils remain oxic post-thaw.

4.3. Incubation derived rates to quantify permafrost C loss

The limited contribution from permafrost sources to surface flux using our *in situ* $^{14}CO_2$ flux measurements became even more notable when compared with the contribution estimated using anoxic CO_2 production rates from laboratory incubations. In agreement with other anoxic incubation data (Treat et al., 2015), we did observe decreasing decomposition rates with depth in our incubations, reflecting the greater levels of degradation of the organic matter in the permafrost. However, given the large amounts of SOC that were exposed to

decomposition after the collapse, using these incubations we estimated that the contribution from previously-frozen C at depth should have been between 25 and 47% of surface fluxes and much greater than our field observations from radiocarbon measurements (Table S4). This divergence is also critical as predictions of permafrost C release are currently based on production rates derived from incubations (Koven et al., 2015) and may thus represent a substantial overestimate for anoxic soils. Our incubation and field results suggest that there are fundamental differences in the conditions under which organic matter decomposition takes place in incubations versus *in situ*. Incubations poorly represent the concentration gradients of end products of decomposition and rates of diffusive transport occurring *in situ* in peat profiles (Elberling et al., 2011). The total CO_2 or CH_4 produced (potential production rates) is assumed to be transported and released at the same rate it is produced, which potentially results in an overestimation of the contribution of deeper layers to surface fluxes. Additionally, the accumulation of large pools of end products of decomposition is argued to limit further decay thermodynamically in anoxic systems (Beer and Blodau, 2007; Blodau et al., 2011). This, together with the accumulation of inhibitory compounds (e.g. phenolics (Freeman et al., 2004)), could help explain why *in situ* rates of decomposition at depth appear to be much lower than potential rates of activity measured under laboratory conditions, often following transport and preparation periods during which peats were exposed to oxygen. The possible overestimation of decomposition rates in anaerobic incubations suggests the importance of oxic conditions in promoting the release of previously-frozen C may be even greater than previously considered, at least in the case of our studied peatlands.

4.4. Soil C balance and radiative forcing in collapsing peatlands

Our soil C balance estimates indicate that thermokarst in peat plateaus increased the landscape C sink for several decades and that the strength of this effect decreased with time following thaw (Fig. 8a). A limitation of our C balance estimates is that it assumes that the lack of permafrost C loss detected in our single year of measurement applies to the entire period since thaw. However, we selected sites that collapsed between ~20 and ~100 yr ago and investigated actively-thawing
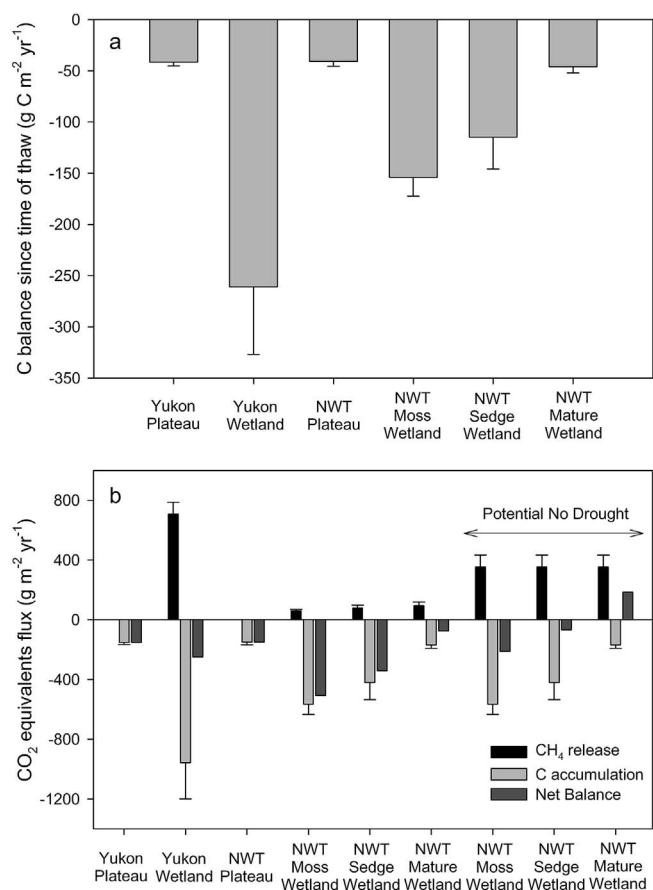
Fig. 8. Estimates of carbon and CO$_2$ equivalents balance in peatland plateaus and collapse wetlands in Yukon and NWT over the time since thaw period. Panel (a) shows the mean C balance estimated from the difference between C accumulation rates since thaw and the negligible respiration from permafrost sources. Error bars represent ± s.e.m. Negative values indicate C gains by the soils. Panel (b) shows the balance of CO$_2$ equivalents flux calculated from the difference of CH$_4$ release (CO$_2$ equivalents over 100 yr period, 1 kg CH$_4$ = 34 kg CO$_2$ equivalent) and CO$_2$ uptake from C accumulation rates over the time since thaw period. Positive values indicate CO$_2$ equivalents input to the atmosphere. Error bars for the CH$_4$ release and C accumulation components represent ± s.e.m. The effect of drought on CH$_4$ flux in the NWT wetlands was reduced by assuming those wetlands released half of the CH$_4$ released from the Yukon wetland in a non-dry year (Potential No Drought). See Table S5 for calculations and ratios of CH$_4$ release to CO$_2$ uptake (Frolking et al., 2006).

edges (Margin in the Yukon wetland) but could not detect a contribution of permafrost C sources to CO$_2$ release under any of these conditions. Given the limited *in situ* release of previously-frozen C as either CO$_2$ (Fig. 4) or CH$_4$ (Cooper et al., 2017) in our collapse wetlands, the increased C sink function was mostly driven by the rapid C gain in surface peats following thaw (Fig. 6). Our post-thaw C accumulation rates in collapse wetlands (Fig. 7) agree with reported values of between 169 and 318 g C m^{-2} yr^{-1} in Manitoba (Camill, 1999) and between as little as 12 and as much as 508 g C m^{-2} yr^{-1} in Alaska (Jones et al., 2016), while much greater C accumulation rates of the order of few thousands of g C m^{-2} yr^{-1} have been reported after thaw in Alberta (Wilson et al., 2017). In agreement with these studies and others (Turetsky et al., 2007), we observed the rate of accumulation post-thaw to also decline with time (Fig. 7b), but we further noted the rate to be strongly related to the depth of collapse, with greatest accumulation in the deepest subsided ground (Fig. 7a). We speculate that depth of collapse is positively related to ground ice content in peat plateaus, and that the greater the ground subsidence, the greater depth of inundation (deeper water column above the subsided ground). This implies a larger volume that can be filled by new peat before the system starts to become drier, resulting in sustained high C accumulation rates over a

longer time period.

The potential control of the depth of collapse on post-thaw C accumulation (Fig. 7a) may also determine the impact of thaw in peatlands on radiative forcing. We observed C sequestration to outweigh substantial CH$_4$ release thus resulting in a net cooling effect relative to the plateau in Yukon, our deepest collapse. In our relatively young wetlands, collapsed within the last 100 yr, we observed the potential cooling effect to decrease with time since thaw and increasing CH$_4$ release to CO$_2$ uptake ratios (mol:mol, Table S5). In the longer-term, it is expected that CH$_4$ fluxes should also decrease with time since thaw (Johnston et al., 2014), as peat starts accumulating above the water table (Camill, 1999). However, the extent of such reduction is likely controlled by local hydrological and surface subsidence conditions (Olefeldt et al., 2013) and, thus, improved information on the spatial variability of permafrost ice content is first required. Ultimately, in our studied sites it appears that there may be a net cooling effect during the most rapid period of new peat production in the first few decades after thaw, and that CH$_4$ emission may then become increasing important in the medium-term (several decades), but in the longer term it has been suggested that increased peat production will likely dominate feedback at the multi-century timescale (Frolking et al., 2006; Wilson et al., 2017). Improving understanding of the timelines of peat production versus the release of CH$_4$ is important if we are to predict the magnitude of the permafrost feedback for policy-relevant periods of the 21st century.

5. Conclusion

We studied fire-induced permafrost thaw in well-drained forests sites and thaw resulting in the formation of collapse wetlands in peatland sites. Overall, our research demonstrates that in our studied ecosystems, oxic conditions are required for substantial C losses from previously-frozen SOC after permafrost thaw. While deep C stocks contributed to surface fluxes in almost all oxic sites, and very substantially in one burnt forest plot, we could not detect CO$_2$ release from previously-frozen C under anoxic conditions. This was the case even where peat C stocks were substantial and anoxic incubation data indicated that previously-frozen layers should contribute up to 50% of total fluxes. Furthermore, the rapid formation of new peat following thaw in collapse wetlands resulted in net C uptake. In our sites, this negative radiative forcing feedback appeared to be greater in magnitude than the positive radiative forcing feedback associated with CH$_4$ release. While there remains considerable uncertainty regarding the relative magnitudes of these two feedbacks, greater rates of new peat formation have the potential to offset a substantial proportion of the increased CH$_4$ emissions from thawing peatlands. Our findings emphasise that determining the effects of permafrost thaw on landscape wetness is therefore key for predicting the sign and magnitude of the permafrost C feedback to climate change in different ecosystems. Finally, these results from our studied peatlands have important implications for models representing anaerobic decomposition since current predictions based on incubations may overestimate rates of permafrost C release compared with *in situ* measurements.

Data availability

The data used in this article are available through the Environmental Information Data Centre (EIDC) hosted by the Centre for Ecology and Hydrology (CEH) and Natural Environment Research Council (NERC) and has been assigned the data identifier https://catalogue.ceh.ac.uk/documents/108ed94d-3385-4e54-ba96-d4ad387fcae1.

The radiocarbon data, together with the laboratory codes, are presented in the supplementary material.

Acknowledgements

We thank Yukon College and Aurora Geosciences Ltd. and to Bronwyn Benkert and Dave White for coordination in logistical support. This work was funded by the UK Natural Environment Research Council (NERC) through grants to I.P.Hartley [NE/K000179/1], to G.K.Phoenix [NE/K00025X/1], to J.B.Murton [NE/K000241/1], to M.Williams [NE/K000292/1], and a University of Sheffield Righ Foundation Studentship to R.Treharne. The authors have no competing interests to declare.

Appendix A. Supplementary data

Supplementary data related to this article can be found at http://dx.doi.org/10.1016/j.soilbio.2017.12.010.

References

Appleby, P.G., 2001. Chronostratigraphic techniques in recent sediments. In: Last, W.M., Smol, J.P. (Eds.), Tracking Environmental Change Using Lake Sediments Volume 1: Basin Analysis, Coring and Chronological Techniques. Klower Academic Publishers, Dordrecht.

Beer, J., Blodau, C., 2007. Transport and thermodynamics constrain belowground carbon turnover in a Northern Peatland. Geochimica et Cosmochimica Acta 71, 2989–3002. http://dx.doi.org/10.1016/j.gca.2007.03.010.

Beilman, D.W., 2001. Plant community and diversity change due to localized permafrost dynamics in bogs of Western Canada. Canadian Journal of Botany 79, 983–993. http://dx.doi.org/10.1139/cjb-79-8-983.

Blodau, C., Siems, M., Beer, J., 2011. Experimental burial inhibits methanogenesis and anaerobic decomposition in water-saturated peats. Environmental Science and Technology 45, 9984–9989. http://dx.doi.org/10.1021/es201777u.

Brown, J., Ferrians, O.J., Heginbottom, J.A., Melnikov, E.S., 1997. Circum-arctic Map of Permafrost and Ground-ice Conditions. Circum-Pacific Map Series. U.S. Geological Survey, Washington, D.C.

Brown, J., Romanovsky, V.E., 2008. Report from the international permafrost association: state of permafrost in the first decade of the 21st century. Permafrost and Periglacial Processes 19, 255–260. http://dx.doi.org/10.1002/ppp.618.

Burn, C.R., 1998. The response (1958-1997) of permafrost and near-surface ground temperatures to forest fire, Takhini River Valley, Southern Yukon Territory. Canadian Journal of Earth Sciences 35, 184–199. http://dx.doi.org/10.1139/e97-105.

Camill, P., 2005. Permafrost thaw accelerates in boreal peatlands during late-20th century climate warming. Climatic Change 68, 135–152. http://dx.doi.org/10.1007/s10584-005-4785-y.

Camill, P., 1999. Peat accumulation and succession following permafrost thaw in the boreal peatlands of Manitoba, Canada. Ecoscience 6, 592–602. http://dx.doi.org/10.1080/11956860.1999.11682561.

Chasmer, L., Kenward, A., Quinton, W., Petrone, R., 2012. CO2 exchanges within zones of rapid conversion from permafrost plateau to bog and fen land cover types. Arctic Antarctic and Alpine Research 44, 399–411. http://dx.doi.org/10.1657/1938-4246-44.4.399.

Ciais, P., Sabine, C., Bala, G., Bopp, L., Brovkin, V., Canadell, J., Chhabra, A., DeFries, R., Galloway, J., Heimann, M., Jones, C., Quéré, C. Le, Myneni, R.B., Piao, S., Thornton, P., 2013. The physical science basis. In: Contribution of Working Group I to the Fifth Assessment Report of the Intergovernmental Panel on Climate Change. IPCC Climate Change, pp. 465–570. http://dx.doi.org/10.1017/CBO9781107415324.015.

Clague, J.J., Evans, S.G., Rampton, V.N., Woodsworth, G.J., 1995. Improved age estimates for the White River and Bridge River Tephras, Western Canada. Canadian Journal of Earth Sciences 32, 1172–1179. http://dx.doi.org/10.1139/e95-096.

Cooper, M.D.A., Estop-Aragonés, C., Fisher, J.P., Thierry, A., Garnett, M.H., Charman, D.J., Murton, J.B., Phoenix, G.K., Treharne, R., Kokelj, S.V., Wolfe, S.A., Lewkowicz, A.G., Williams, M., Hartley, I.P., 2017. Limited contribution of permafrost carbon to methane release from thawing peatlands. Nature Climate Change 7, 507–511. http://dx.doi.org/10.1038/NCLIMATE3328.

Elberling, B., Askaer, L., Jørgensen, C.J., Joensen, H.P., Kühl, M., Glud, R.N., Lauritsen, F.R., 2011. Linking soil O2, CO2, and CH4 concentrations in a wetland soil: implications for CO2 and CH4 fluxes. Environmental Science and Technology 45, 3393–3399.

Environment Canada, 2015. Climate Data Online. http://climate.weather.gc.ca/climate_normals, Accessed date: 17 May 2017.

Estop-Aragonés, C., Knorr, K.H., Blodau, C., 2012. Controls on in situ oxygen and dissolved inorganic carbon dynamics in peats of a temperate fen. Journal of Geophysical Research: Biogeosciences 117, 1–14. http://dx.doi.org/10.1029/2011JG001888.

Euskirchen, E.S., Edgar, C.W., Turetsky, M.R., Waldrop, M.P., Harden, J.W., 2014. Differential response of carbon fluxes to climate in three peatland ecosystems that vary in the presence and stability of permafrost. Journal of Geophysical Research: Biogeosciences 119, 1576–1595. http://dx.doi.org/10.1002/2013JG002433.

Fisher, J.P., Estop-Aragonés, C., Thierry, A., Charman, D.J., Wolfe, S.A., Hartley, I.P., Murton, J.B., Williams, M., Phoenix, G.K., 2016. The influence of vegetation and soil characteristics on active-layer thickness of permafrost soils in boreal forest. Global Change Biology 22, 3127–3140. http://dx.doi.org/10.1111/gcb.13248.

Freeman, C., Ostle, N.J., Fenner, N., Kang, H., 2004. A regulatory role for phenol oxidase

during decomposition in peatlands. Soil Biology and Biochemistry 36, 1663–1667. http://dx.doi.org/10.1016/j.soilbio.2004.07.012.

Frolking, S., Roulet, N., Fuglestvedt, J., 2006. How northern peatlands influence the earth's radiative budget: sustained methane emission versus sustained carbon sequestration. Journal of Geophysical Research: Biogeosciences 111, 1–10. http://dx.doi.org/10.1029/2005JG000091.

Garnett, M.H., Hardie, S.M.L., 2009. Isotope (14C and 13C) analysis of deep peat CO2 using a passive sampling technique. Soil Biology and Biochemistry 41, 2477–2483. http://dx.doi.org/10.1016/j.soilbio.2009.09.004.

Garnett, M.H., Hartley, I.P., Hopkins, D.W., Sommerkorn, M., Wookey, P.A., 2009. A passive sampling method for radiocarbon analysis of soil respiration using molecular sieve. Soil Biology and Biochemistry 41, 1450–1456. http://dx.doi.org/10.1016/j.soilbio.2009.03.024.

Gillett, N.P., Weaver, A.J., Zwiers, F.W., Flannigan, M.D., 2004. Detecting the effect of climate change on Canadian forest fires. Geophysical Research Letters 31. http://dx.doi.org/10.1029/2004GL020876.

Gorham, E., Lehman, C., Dyke, A., Janssens, J., Dyke, L., 2007. Temporal and spatial aspects of peatland initiation following deglaciation in North America. Quaternary Science Reviews 26, 300–311. http://dx.doi.org/10.1016/j.quascirev.2006.08.008.

Grosse, G., Harden, J., Turetsky, M., McGuire, A.D., Camill, P., Tarnocai, C., Frolking, S., Schuur, E.A.G., Jorgenson, T., Marchenko, S., Romanovsky, V., Wickland, K.P., French, N., Waldrop, M., Bourgeau-Chavez, L., Striegl, R.G., 2011. Vulnerability of high-latitude soil organic carbon in North America to disturbance. Journal of Geophysical Research: Biogeosciences 116, 1–23. http://dx.doi.org/10.1029/2010JG001507.

Harden, J.W., Sundquist, E.T., Stallard, R.F., Mark, R.K., 1992. Dynamics of soil carbon during deglaciation of the Laurentide ice sheet. Science 258, 1921–1924.

Harden, J.W., Koven, C.D., Ping, C.L., Hugelius, G., David McGuire, A., Camill, P., Jorgenson, T., Kuhry, P., Michaelson, G.J., O'Donnell, J.A., Schuur, E.A.G., Tarnocai, C., Johnson, K., Grosse, G., 2012. Field information links permafrost carbon to physical vulnerabilities of thawing. Geophysical Research Letters 39, 1–6. http://dx.doi.org/10.1029/2012GL051958.

Helbig, M., Chasmer, L.E., Desai, A.R., Kljun, N., Quinton, W.L., Sonnentag, O., 2017. Direct and indirect climate change effects on carbon dioxide fluxes in a thawing boreal forest-wetland landscape. Global Change Biology 3231–3248. http://dx.doi.org/10.1111/gcb.13638.

Hugelius, G., Strauss, J., Zubrzycki, S., Harden, J.W., Schuur, E.A.G., Ping, C.L., Schirrmeister, L., Grosse, G., Michaelson, G.J., Koven, C.D., O'Donnell, J.A., Elberling, B., Mishra, U., Camill, P., Yu, Z., Palmtag, J., Kuhry, P., 2014. Estimated stocks of circumpolar permafrost carbon with quantified uncertainty ranges and identified data gaps. Biogeosciences 11, 6573–6593. http://dx.doi.org/10.5194/bg-11-6573-2014.

Johnston, C.E., Ewing, S.A., Harden, J.W., Varner, R.K., Wickland, K.P., Koch, J.C., Fuller, C.C., Manies, K., Jorgenson, M.T., 2014. Effect of permafrost thaw on CO2 and CH4 exchange in a Western Alaska peatland chronosequence. Environmental Research Letters 9, 85004. http://dx.doi.org/10.1088/1748-9326/9/8/085004.

Jones, M.C., Harden, J., O'Donnell, J., Manies, K., Jorgenson, T., Treat, C., Ewing, S., 2016. Rapid carbon loss and slow recovery following permafrost thaw in boreal peatlands. Global Change Biology. http://dx.doi.org/10.1111/gcb.13403.

Jorgenson, M.T., Osterkamp, T.E., 2005. Response of boreal ecosystems to varying modes of permafrost degradation. Canadian Journal of Forest Resources 35, 2100–2111. http://dx.doi.org/10.1139/X05-153.

Kasischke, E.S., Verbyla, D.L., Rupp, S., McGuire, D., Murphy, K.A., Jandt, R., Barnes, J.L., Hoy, E.E., Duffy, P.A., Calef, M., Turetsky, M.R., 2010. Alaska's changing fire regime — implications for the vulnerability of its boreal forests. Canadian Journal of Forest Research 40, 1302–1312. http://dx.doi.org/10.1139/X10-061.

Koven, C.D., Ringeval, B., Friedlingstein, P., Ciais, P., Cadule, P., Khvorostyanov, D., Krinner, G., Tarnocai, C., 2011. Permafrost carbon-climate feedbacks accelerate global warming. Proceedings of the National Academy of Sciences of the United States of America 108, 14769–14774. http://dx.doi.org/10.1073/pnas.1103910108.

Koven, C.D., Schuur, E.A.G., Schädel, C., Bohn, T.J., Burke, E.J., Chen, G., Chen, X., Ciais, P., Grosse, G., Harden, J.W., Hayes, D.J., Hugelius, G., Jafarov, E.E., Krinner, G., Kuhry, P., Lawrence, D.M., MacDougall, A.H., Marchenko, S.S., McGuire, A.D., Natali, S.M., Nicolsky, D.J., Olefeldt, D., Peng, S., Romanovsky, V.E., Schaefer, K.M., Strauss, J., Treat, C.C., Turetsky, M., 2015. A simplified, data-constrained approach to estimate the permafrost carbon–climate feedback. Philosophical Transactions of the Royal Society A: Mathematical, Physical & Engineering Sciences 373, 20140423. http://dx.doi.org/10.1098/rsta.2014.0423.

Levin, I., Kromer, B., Hammer, S., 2013. Atmospheric δ14CO2 trend in Western European background air from 2000 to 2012. Tellus, Series B: Chemical and Physical Meteorology 65, 1–7. http://dx.doi.org/10.3402/tellusb.v65i0.20092.

Lewkowicz, A.G., Etzelmüller, B., Smith, S.L., 2011. Characteristics of discontinuous permafrost based on ground temperature measurements and electrical resistivity tomography, Southern Yukon, Canada. Permafrost and Periglacial Processes 22, 320–342. http://dx.doi.org/10.1002/ppp.703.

Livingston, G., Hutchinson, G., Matson, P.A., Harriss, R., 1995. Enclosure-based measurement of trace gas exchange: applications and sources of error. In: Biogenic Trace Gases: Measuring Emissions from Soil and Water, vol. 51. Blackwell Publishing, Oxford, UK, pp. 14–51.

Mackay, J.R., 1981. Active layer slope movement in a continuous permafrost environment, Garry Island, Northwest Territories, Canada. Canadian Journal of Earth Sciences 18, 1666–1680. http://dx.doi.org/10.1139/e81-154.

Mackay, J.R., 1958. A Subsurface Organic Layer Associated with Permafrost in the Western Arctic. Geographical Branch, Department of Mines and Technical Surveys, Ottawa, ON, pp. 18–21 Geographical Paper.

McGuire, A.D., Koven, C., Lawrence, D.M., Clein, J.S., Xia, J., Beer, C., Burke, E., Chen, G.,

Chen, X., Delire, C., Jafarov, E., MacDougall, Andrew H., SM, Nicolsky, D., Peng, S., Rinke, A., Saito, K., Zhang, W., Alkama, R., Bohn, T.J., Ciais, P., Decharme, B., Ekici, A., Gouttevin, I., Hajima, T., Hayes, D.J., Ji, D., Krinner, G., Lettenmaier, D.P., Luo, Y., Miller, P.A., Moore, J.C., Romanovsky, V., Schädel, C., Schaefer, K., Schuur, E.A.G., Smith, B., Sueyoshi, T., Zhuang, Q., 2016. Variability in the sensitivity among model simulations of permafrost and carbon dynamics in the permafrost region between 1960 and 2009. Global Biogeochemical Cycles 30, 1015–1037. http://dx.doi.org/10.1002/2016GB005405.

Morse, P.D., Wolfe, S.A., Kokelj, S.V., Gaanderse, A.J.R., 2016. The occurrence and thermal disequilibrium state of permafrost in forest ecotopes of the Great Slave Region, Northwest Territories, Canada. Permafrost and Periglacial Processes 27, 145–162. http://dx.doi.org/10.1002/ppp.1858.

Myhre, G., Shindell, D., Bréon, F.-M., Collins, W., Fuglestvedt, J., Huang, J., Koch, D., Lamarque, J.-F., Lee, D., Mendoza, B., Nakajima, T., Robock, A., Stephens, G., Takemura, T., Zhang, H., 2013. Anthropogenic and natural radiative forcing. In: Climate Change 2013: The Physical Science Basis. Contribution of Working Group I to the Fifth Assessment Report of the Intergovernmental Panel on Climate Change, pp. 659–740. http://dx.doi.org/10.1017/CBO9781107415324.018.

O'Donnell, J.A., Jorgenson, M.T., Harden, J.W., McGuire, A.D., Kanevskiy, M.Z., Wickland, K.P., 2012. The effects of permafrost thaw on soil hydrologic, thermal, and carbon dynamics in an alaskan peatland. Ecosystems 15, 213–229. http://dx.doi.org/10.1007/s10021-011-9504-0.

Olefeldt, D., Turetsky, M.R., Crill, P.M., Mcguire, A.D., 2013. Environmental and physical controls on northern terrestrial methane emissions across permafrost zones. Global Change Biology 19, 589–603. http://dx.doi.org/10.1111/gcb.12071.

Osterkamp, T.E., Viereck, L., Shur, Y., Jorgenson, M.T., Racine, C., Doyle, A., Boone, R.D., 2000. Observations of thermokarst and its impact on boreal forests in Alaska, USA. Arctic, Antarctic, and Alpine Research 32, 303–315. http://dx.doi.org/10.2307/1552529.

Rand, J., Mellor, M., 1985. Ice-coring Augers for Shallow Depth Sampling. U.S. Army Cold Regions Research and Engineering Laboratory, Hanover, New Hampshire 27.

Robinson, S.D., 2001. Extending the late Holocene White River Ash distribution, Northwestern Canada. Arctic 54, 157–161.

Robinson, S.D., Moore, T.R., 2000. The influence of permafrost and fire upon carbon accumulation in high boreal peatlands, Northwest Territories, Canada. Arctic Antarctic and Alpine Research 32, 155–166. http://dx.doi.org/10.2307/1552447.

Schädel, C., Bader, M.K.-F., Schuur, E.A.G., Biasi, C., Bracho, R., Čapek, P., De Baets, S., Diáková, K., Ernakovich, J., Estop-Aragones, C., Graham, D.E., Hartley, I.P., Iversen, C.M., Kane, E., Knoblauch, C., Lupascu, M., Martikainen, P.J., Natali, S.M., Norby, R.J., O'Donnell, J.A., Chowdhury, T.R., Šantrůčková, H., Shaver, G., Sloan, V.L., Treat, C.C., Turetsky, M.R., Waldrop, M.P., Wickland, K.P., 2016. Potential carbon emissions dominated by carbon dioxide from thawed permafrost soils. Nature Climate Change 6, 1–5. http://dx.doi.org/10.1038/nclimate3054.

Schaefer, K., Lantuit, H., Romanovsky, V.E., Schuur, E. a G., Witt, R., 2014. The impact of the permafrost carbon feedback on global climate. Environmental Research Letters 9, 85003. http://dx.doi.org/10.1088/1748-9326/9/8/085003.

Schuur, E.A.G., McGuire, A.D., Grosse, G., Harden, J.W., Hayes, D.J., Hugelius, G., Koven, C.D., Kuhry, P., 2015. Climate change and the permafrost carbon feedback. Nature 520, 171–179. http://dx.doi.org/10.1038/nature14338.

Schuur, E.A.G., Vogel, J.G., Crummer, K.G., Lee, H., Sickman, J.O., Osterkamp, T.E., 2009. The effect of permafrost thaw on old carbon release and net carbon exchange from tundra. Nature 459, 556–559. http://dx.doi.org/10.1038/nature08031.

Stuiver, M., Polach, H., 1977. Reporting of Radiocarbon Data, vol. 19. pp. 355–363.

Tarnocai, C., Canadell, J.G., Schuur, E.A.G., Kuhry, P., Mazhitova, G., Zimov, S., 2009. Soil Organic Carbon Pools in the Northern Circumpolar Permafrost Region, vol. 23. pp. 1–11. http://dx.doi.org/10.1029/2008GB003327.

Treat, C.C., Natali, S.M., Ernakovich, J., Iversen, C.M., Lupascu, M., Mcguire, A.D., Norby, R.J., Roy Chowdhury, T., Richter, A., Šantrůčková, H., Schädel, C., Schuur, E.A.G., Sloan, V.L., Turetsky, M.R., Waldrop, M.P., 2015. A pan-arctic synthesis of CH4 and CO2 production from anoxic soil incubations. Global Change Biology 21, 2787–2803. http://dx.doi.org/10.1111/gcb.12875.

Turetsky, M.R., Manning, S.W., Wieder, R.K., 2004. Dating recent peat deposits. Wetlands 24, 324–356.

Turetsky, M.R., Wieder, R.K., Vitt, D.H., 2002. Boreal peatland C fluxes under varying permafrost regimes. Soil Biology and Biochemistry 34, 907–912. http://dx.doi.org/10.1016/S0038-0717(02)00022-6.

Turetsky, M.R., Wieder, R.K., Vitt, D.H., Evans, R.J., Scott, K.D., 2007. The disappearance of relict permafrost in boreal north America: effects on peatland carbon storage and fluxes. Global Change Biology 13, 1922–1934. http://dx.doi.org/10.1111/j.1365-2486.2007.01381.x.

Turetsky, M.R., Wieder, R.K., Williams, C.J., Vitt, D.H., 2000. Organic matter accumulation, peat chemistry, and permafrost melting in peatlands of boreal Alberta. Ecoscience 7, 379–392. http://dx.doi.org/10.1080/11956860.2000.11682608.

Walter Anthony, K., Daanen, R., Anthony, P., Schneider Von Deimling, T., Ping, C.L., Chanton, J.P., Grosse, G., 2016. Methane emissions proportional to permafrost carbon thawed in Arctic lakes since the 1950s. Nature Geoscience 9, 679–682. http://dx.doi.org/10.1038/ngeo2795.

Wickland, K.P., Striegl, R.G., Neff, J.C., Sachs, T., 2006. Effects of permafrost melting on CO2 and CH4 exchange of a poorly drained black spruce lowland. Journal of Geophysical Research: Biogeosciences 111, 1–13. http://dx.doi.org/10.1029/2005JG000099.

Wilson, R.M., Fitzhugh, L., Whiting, G.J., Frolking, S., Harrison, M.D., Dimova, N., Burnett, W.C., Chanton, J.P., 2017. Greenhouse gas balance over thaw-freeze cycles in discontinuous zone permafrost. Journal of Geophysical Research: Biogeosciences 1–18. http://dx.doi.org/10.1002/2016JG003600.

Wilson, R.M., Hopple, A.M., Tfaily, M.M., Sebestyen, S.D., Schadt, C.W., Pfeifer-Meister, L., Medvedeff, C., Mcfarlane, K.J., Kostka, J.E., Kolton, M., Kolka, R.K., Kluber, L.A., Keller, J.K., Guilderson, T.P., Griffiths, N.A., Chanton, J.P., Bridgham, S.D., Hanson, P.J., 2016. Stability of peatland carbon to rising temperatures. Nature Communications 7, 13723. http://dx.doi.org/10.1038/ncomms13723.

Wolfe, S.A., Morse, P.D., 2016. Lithalsa formation and Holocene lake-level recession, Great Slave Lowland, Northwest Territories. Permafrost and Periglacial Processes. http://dx.doi.org/10.1002/ppp.1901.

Yoshikawa, K., Bolton, W.R., Romanovsky, V.E., Fukuda, M., Hinzman, L.D., 2002. Impacts of wildfire on the permafrost in the boreal forests of Interior Alaska. Journal of Geophysical Research 108, 16–17. http://dx.doi.org/10.1029/2001JD000438.

Zoltai, S.C., 1995. Permafrost distribution in peatlands of West-Central Canada during the Holocene warm period 6000 years BP. Geographie Physique Et Quaternaire 49, 45–54. http://dx.doi.org/10.7202/033029ar.

Zoltai, S.C., 1993. Cyclic development of permafrost in the peatlands of Northwestern Canada. Arctic & Alpine Research 25, 240–246. http://dx.doi.org/10.2307/1551820.